REPORT No. 96

THE DEVELOPMENT OF A PERTURBED, INCOMPRESSIBLE, TURBULENT BOUNDARY LAYER

by
HISAYUKI HANDA

January 1969

GAS TURBINE LABORATORY
MASSACHUSETTS INSTITUTE OF TECHNOLOGY
CAMBRIDGE, MASSACHUSETTS 02139

THE DEVELOPMENT OF A PERTURBED, INCOMPRESSIBLE, TURBULENT BOUNDARY LAYER

by

HISAYUKI HANDA

Under the Sponsorship of:

General Electric Company

Allison Division of General Motors Company

GAS TURBINE LABORATORY

REPORT No. 96

January 1969

MASSACHUSETTS INSTITUTE OF TECHNOLOGY

Cambridge, Massachusetts

ABSTRACT

The response of a fully-developed equilibrium turbulent boundary layer to a small disturbance was observed experimentally under low-Mach-number conditions: a turbulent boundary layer in an axisymmetric channel under zero pressure gradient was perturbed by a single fencelike two-dimensional protuberance, and the subsequent development of the velocity profile, the turbulent-shear-stress profile, and the wall shear stress was recorded by a constant-temperature hot-wire anemometer and a Preston tube. The height of the five roughness elements used ranged from 0.011 to 0.100 inches (2-15% of the original boundary layer thickness).

The perturbation effects are observable only in the vicinity of their origin and each parameter undergoes an individual recovery process. The wall shear stress exhibits a unique style in its development. A perturbed turbulent-shear-stress profile shows a maximum as in the case of a turbulent boundary layer in an adverse pressure gradient. The analysis of the data has revealed a self-preserving feature of the developing velocity profile in form for small enough disturbances: the wall region of the boundary layer is in a local equilibrium after 30 roughness-heights and the unaffected outer layer retains its original characteristics.

ACKNOWLEDGEMENTS

First of all, my sincerest and deepest gratitude to Professor Edward S. Taylor who allowed me the opportunity of being a research assistant at the Gas Turbine Laboratory. This past year has been most educational in every respect and this experience made me not only a better engineer but also a better man.

My appreciation to Professor David G. Wilson who conceived the original project and whose advice, encouragement and constant concern enabled me to complete this work.

Thoughtful comments of the members of my "thesis review committee", especially of Prof. J. L. Kerrebrock and Dr. M. P. Escudier, are gratefully acknowledged.

No work at the G.T.L. can proceed smoothly without the humour and ever-ready helpful hands of Mr. Thorwald Christensen. He is the only remedy for the consequences of the fact stated in "Murphy's law". I express my thanks to him here.

It was my great pleasure to have been acquainted with all the members of the G.T.L. I am grateful to their companionship, friendly advice and assistance which made miserable times bearable and which helped me to endure the vigour of graduate life at M.I.T.: especially, I would like to acknowledge the help of Mrs. Lotte Gopalakrishnan who typed this report and whose coffee (certainly the America's best!) woke me up in the morning and kept me alert till late at night solely to prolong my working hours.

Lastly, I would like to thank my host-family [Mr. & Mrs. Earl A. Williams, Ricky and Tina], my parents, my brother and my sister for everything.

TABLE OF CONTENTS

LIST OF FIGURES

NOMENCLATURE

A, B	constants
C_f	skin friction coefficient
d	diameter
f, F	Functions defined in Eq. (1) and (2)
h	roughness height
H	$\frac{\delta^*}{\theta}$: shape factor
k	von Karman constant
p	pressure
$\overline{u}$	time-average velocity in x direction
u', v'	velocity fluctuation in x and y directions
U_∞	free-stream velocity at x = o
u_*	wall friction velocity
$\frac{\Delta u}{u_*}$	roughness parameter in Eq. (8)
$\overline{v}$	time-average velocity at the edge of the internal boundary layer
v_*	$\frac{\tau}{\rho}$ at the edge of the internal boundary layer
x, y	spacial coordinates
x_0	location of roughness elements
W	Coles' wake function
β	$\frac{\delta^*}{\tau_w}\frac{dp}{dx}$
η	y/δ : non-dimensionalized y coordinate
δ	boundary layer thickness
δ_{in}	thickness of internal boundary layer

δ^*	displacement thickness
θ	momentum thickness
ρ	density
ν	kinematic viscosity
τ_w	wall shear stress

I. INTRODUCTION

A. Motivation to the Project

The fluid dynamics of turbomachinery is one of the most intricate phenomena and carries a great importance in technological development; though our endeavour for its comprehension has not been completely futile, our knowledge is still very much limited; for instance, present design techniques for turbomachinery may be described as a "black art". As the field of application for the machinery continues to expand from electric-power generation, exhaust-gas utilization, to V/STOL power plants, further complications are added to the complexity; the so-called "contour-change" problem of compressor and turbine blades due to erosion and fouling is a typical example.

One of the biggest obstacles in understanding of the fluid dynamics in a rotating machine is the lack of knowledge in the behavior of a boundary layer under various environmental conditions - phenomena like laminar-turbulent transition, laminar and turbulent separation, and roughness effects: especially, turbulent boundary layers, unlike laminar ones, are quite difficult to analyse theoretically.

Although there exist several practical solutions to the contour-change problem, these contain intrinsically undesirable features and must be considered as temporary. Therefore, in the quest for a better solution and in promoting the understanding of these problems and the fluid dynamics of turbomachinery in general, the study of the perturbed turbulent boundary layer, with a simplified model of dust particles and surface roughnesses as the cause of perturbations, occupies an important position.

Fairly successful potential theories in the prediction of airfoil characteristics assist our search for comprehension of fluid dynamics of turbomachinery - the potential theory with conformal mapping by T. Theodorsen & I. E. Garrick [Ref. 7] and the singularity method developed by H. Schlichting [Ref. 4]. The shortcoming of these theories, however, arises from the assumption of the Kutta condition (no wake-effect consideration on airfoil-circulation determination) and the neglect of viscosity. The former, however, was shown to have only a minor effect by J. H. Preston & E. C. Maskell [Ref. 3]. Various improvements have been achieved by P. M. Pinkerton [Ref. 2], D. A. Spence [Ref. 6] and K. H. Schneider [Ref. 5], and the method used by the last author predicted airfoil lift coefficients within 3% of the experimental value, which was better than any previous work. Schneider modified the "thin-airfoil theory" and applied Schlichting's sigularity method to an "effective body contour" defined by addition of the experimentally determined displacement thickness of the boundary layer to the base thickness form. In the analytical treatment, this effective body was represented by sinks and sources, and the camber line by distributed vortices. The distribution of these singularities was assumed to be in the form of an infinite trigonometric series with adjustable coefficients, following Glauert's approach. The number of boundary conditions (slope of effective contour) fixed the number of determinable coefficients. An additional improvement was brought about by retaining a usually neglected second-order term in the continuity equation.

Hence, Schneider's method being available, the theoretical analysis of the contour-change problem reduces to an accurate boundary-layer-

characteristic prediction. Though the investigations concerning laminar separation and possible subsequent turbulent reattachment, laminar-to-turbulent transition due to roughnesses in the vicinity of the leading edge of an airfoil or a compressor blade, turbulent separation, etc., are important, thorough understanding of these phenomena appears to be feasible only in the distant future, simply because the mechanism of turbulence itself escapes our knowledge. Also, the portion of a compressor blade occupied by a laminar boundary layer is usually relatively small compared with that of turbulent one. These considerations indicate the significance of and the immediate need for a further research in the fundamental study of turbulent-boundary-layer development.

In 1956, F. H. Clauser [Ref. 8] described the turbulent boundary layer as a non-linear, dynamic system enclosed in a black box. This non-linearity implies that the turbulent boundary layer possesses a "memory": it is capable of remembering past history. Only recently has the importance of this phenomenon been recognized [see Ref. 13]. Therefore, to ask for a unique universal relationship among local properties like velocity and shear-stress profiles is meaningless except in the case of an "equilibrium" boundary layer which, like a laminar boundary layer, essentially does not remember any history. Consequently, as P. Bradshaw & D. H. Ferris [Ref. 34] mention, initial conditions play a significant role in the <u>development</u> of a turbulent boundary layer: the significance of these initial conditions (or some perturbations upstream) diminishes with downstream distance, finally resulting in only a minor effect like a slightly increased boundary-layer thickness. Since the conditions immediately after the boundary-layer transition from laminar to turbulent,

the method of independent variation of significant parameters at the initial point and those parameters themselves, are unknown, "one is reduced to studying the response of boundary layers to real perturbations, such as might be caused by a region of transpiration or roughness rather than to attempt to generate boundary layers artificially, for instance by vortex generators or graded grids" [Ref. 34]. Therefore, the present project encompasses the general question of turbulent-boundary-layer development as well as the above-mentioned investigation of the contour-change problem due to erosion and fouling in turbomachines. Another application of this study is found in meteorology, where the development of wind-velocity profile in an atmospheric boundary layer after a surface-roughness transition is of interest.

B. Background to the Present Study

A turbulent boundary layer can be conceived as consisting of five imaginary strata: a laminar sublayer where molecular viscosity predominates; a buffer region where turbulent-energy production is most intense; a logarithmic wall region where the transition of molecular to eddy viscosity takes place; a turbulent wake where eddy viscosity predominates; and a superlayer where the entrainment of virtually non-turbulent free-stream fluid into the boundary layer occurs. Though this division is artificial and a turbulent boundary layer should be considered as a single entity or as an integral dynamic system, historically, the stratification has been popular because of its simplicity.

In the theoretical analysis of an incompressible, two-dimensional, turbulent boundary layer in a zero or mild pressure gradient, there exist two so-called "universal similarity laws" - "the law of the wall" for the

inner part of the boundary layer and "the defect law" for the outer part. The former states,

$$\frac{\bar{u}}{u_*} = \text{fcn}\left(\frac{yu_*}{\nu}\right) = f \tag{1}$$

and the latter,

$$\frac{U - \bar{u}}{u_*} = \text{fcn}\,(y/\delta, \pi) = F \tag{2}$$

where π is known to be a function of pressure gradient alone.

In 1954, F. H. Clauser [Ref. 22] made a significant contribution to the field with the discovery of "equilibrium" boundary layers, in which a factor, $\beta \equiv \frac{\delta^*}{\tau_w}\frac{dp}{dx}$, is constant and the afore-mentioned two universal similarity laws hold without qualification. The recent, rigorous study by G. L. Mellor & D. M. Gibson [Ref. 26] has shown the possible existence of equilibrium boundary layers to be for $-0.5 \leq \beta \leq \infty$. H. Ludwieg & W. Tillmann [Ref. 15] experimentally proved the validity of the law of the wall in mild pressure gradients. The defect law is known to hold also for rough surfaces, provided that the origin of y-coordinate is properly chosen, but it is sensitive to free-stream turbulence level.

C. B. A. Millikan showed in 1938 that the velocity profile of the overlapping region of the two universal similarity laws has to be logarithmic. From Eq. (1) and (2),

$$\frac{yu_*}{\nu} f'\,(yu_*/\nu) = \frac{y}{u_*}\frac{\partial \bar{u}}{\partial y} = -\frac{y}{\delta} F'\,(y/\delta) \tag{3}$$

since π is constant for an equilibrium boundary layer. As the two variables, yu_*/ν and y/δ, are independent of each other, each term in

Eq. (3) has to be a constant; let it be 1/k. Then,

$$\frac{yu_*}{\nu} f'(yu_*/\nu) = \frac{1}{k}$$

or,

$$f(yu_*/\nu) = \frac{\bar{u}}{u_*} = \frac{1}{k} \ln \left(\frac{yu_*}{\nu}\right) + A \tag{4}$$

where A is the constant of integration. Coles [Ref. 23] suggests $k = 0.4$ and $A = 5.1$.

In a laminar sublayer, the law of the wall takes the following form:

$$\frac{\bar{u}}{u_*} = \frac{yu_*}{\nu} \tag{5}$$

A single formula for the laminar sublayer, the buffer region and the logarithmic region was found by F. Hama [Ref. 18], G. Kleinstein [Ref. 19] and D. B. Spalding [Ref. 20]. The latter give the formula,

$$y^+ = u^+ + 0.1108 \left[e^{0.4u^+} - 1 - (0.4u^+) - \frac{(0.4u^+)^2}{2!} - \frac{(0.4u^+)^3}{3!} - \frac{(0.4u^+)^4}{4!} \right] \tag{6}$$

where $y^+ \equiv yu_*/\nu$ and $u^+ \equiv \bar{u}/u_*$

By recognizing a similarity between a wake and a turbulent boundary layer and observing that the outer velocity profile to be a mere deviation from the logarithmic profile, D. Coles [Ref. 19] sucessfully extended the law of the wall into the fully turbulent region of the turbulent boundary layer with his "law of the wake":

$$\frac{\bar{u}}{u_*} = \frac{1}{k} \ln \left(\frac{yu_*}{\nu}\right) + A + \frac{\pi}{k} W(\eta) \tag{7}$$

where W is the wake function given in Ref. 19.

An extension of the law of the wall to turbulent boundary layers with rough surfaces have been achieved by various investigators [see Ref. 3, 10, and 30]. Theories generally agree in that the logarithmic profile undergoes a simple linear displacement from that of the smooth wall. Namely.

$$\frac{\bar{u}}{u_*} = \frac{1}{k} \ell n \left(\frac{yu_*}{\nu}\right) + A - \frac{\Delta u}{u_*} \tag{8}$$

where $\frac{\Delta u}{u_*} = \text{fcn}\ (hu_*/\nu)$

For a fully rough surface i.e. $hu_*/\nu \gtrsim 100$, empirically,

$$\frac{\Delta u}{u_*} = \frac{1}{k} \ell n \left(\frac{hu_*}{\nu}\right) + B \tag{9}$$

and Eq. (8) becomes

$$\frac{\bar{u}}{u_*} = \frac{1}{k} \ell n \left(\frac{y}{h}\right) + A - B \tag{10}$$

These analyses have been well verified with J. Nikuradse's experimental data on flows in rough pipes. The similarity between a pipe flow and a channel flow is well established [see Ref. 30].

With these theories, W. P. Elliot, H. A. Panofsky & A. A. Townsend and R. J. Taylor [Ref. 36, 38, 39] have analysed the behavior of turbulent boundary layers in zero pressure gradient after a change in surface roughness, mainly because of meteorological interest in the development of the atmospheric boundary layer which frequently encounters a similar boundary condition. Their analyses utilize the experimentally observed

fact of an internal boundary layer originating in the neighborhood of the surface-roughness transition point. Their mathematical approach is based on the von Karman integral method with Eq. (10) as the assumed velocity profile. Their assumptions such as constant shear stress throughout the boundary layer or linear shear-stress distribution in a distrubed portion of the boundary layer, limit the generalization of the theory, but the method of approach appears to be quite useful. Their prediction of the velocity profile agrees with experimental data only far downstream of the roughness transition point, presumably because of their shear-stress assumptions.

II. EXPERIMENTAL PROGRAM

The experiments were performed at the M.I.T. Gas Turbine Laboratory in order to observe the response of an equilibrium boundary layer to a two-dimensional disturbance. Though some experimental data on this topic exist [see Ref. 1], a complete report on velocity, turbulent-shear-stress and wall-shear-stress development has not been found. Hence, these quantities were measured by a hot-wire anemometer and a Preston tube to obtain a more detailed account of the phenomenon.

A. Modeling

An inherent problem in any study involving a roughness element or a rough surface is the modeling of the actual conditions - roughness shape, density and dimensions in general. This difficulty inevitably introduces uncertainty and lack of generality in the study of protuberance effects. Though Schlichting [Ref. 11] made an attempt to classify protuberance effects and introduced the concept of "equivalent roughness", the variation of shapes and density eliminates any possibility of a completely general classification system.

Under these circumstances, the best compromise is the simplest model; therefore the protuberance chosen here was a two-dimensional fence as shown in Fig. 3. Geometrically, this model is in fact three-dimensional, but as long as the axial length of the protuberance (its thickness) is short enough and the disturbance imposed on the boundary layer is uniform in the transverse direction, the effect may be considered two-dimensional.

Because of the geometry of the test channel (shown in Fig. 2), a ring-type roughness configuration was found to be most appropriate, but

machining of thin sheet metal presented difficulties. The problem was solved with a method which may be described as "trepanning": a gauge-30 aluminum sheet was fixed to a 1/4 inch thick aluminum sheet with contact cement, and the unit was secured on a turn-table on a vertical milling machine; a 1/16 inch diameter tool at high speed was used to cut a ring out of the thinner sheet. This method proved to be successful even for a thickness of 0.008 inch.

The above method was used to machine rings of five different heights - 0.100, 0.077, 0.050, 0.029 and 0.011 inch. These rings were placed on the test channel with a two-sided sticking tape.

B. Apparatus and Instrumentation

The experiments were conducted in an open-circuit wind tunnel shown in Fig. 1. A detailed account of this tunnel is given by P. Goldberg [Ref. 13], so only a brief description is presented here. Atmospheric air is drawn into the tunnel by a radial-inlet, axial-flow fan with the maximum rating of 16000 cfm at 3 inches water static. Then the air goes through several flow-steadying devices, a settling chamber with a honeycomb flow-straightner and a turbulence-reducing silk screen, and finally a 9-to-1 area contraction situated just before the test section. The test channel is axisymmetric, minimizing the possibility of a secondary-flow occurence, and consists of a 10-inch diameter Plexiglas cylinder (shown in Fig. 2) on which a boundary layer grows, and a concentric 24-inch diameter porous metal cylinder used to impose a pressure gradient. Air is exhausted to the atmosphere. Throughout the experiments performed here, the free-stream velocity and the free-stream turbulence intensity at the beginning of the test channel were

approximately 46 ft/sec and 0.2% respectively.

The instrumentation is shown in Fig. 4 through Fig. 6. Atmospheric conditions were measured by a mercury thermometer with an accuracy of $\pm$ 0.5°F and a mercury barometer with an accuracy of $\pm$ 0.01 in Hg. All the pressure measurements except the atmospheric one were taken by a micro-manometer (shown in Fig. 4) manufacutred by R. Hellwig Co., Berlin, West Germany, which is a nulling instrument with methanol as the working fluid; its accuracy is $\pm$ 0.005 mm of the manometer liquid: with methanol, this corresponds to $\pm$ 5.75×10^{-6} psi. The static taps, seen in Fig. 3, are 0.025 inches in diameter: they were machined from 1/8 inch brass plugs and imbedded in the Plexiglas cylinder. A 0.050-inch outside diameter Preston tube, the comparative reliability of which has been demonstrated by P. Goldberg [Ref. 13], was used to obtain the wall shear stress.

Time-mean velocities, velocity fluctuations and turbulent shear stresses were measured by a constant-temperature hot-wire anemometer set shown in Fig. 6; the transistorized amplifier and linearizer were manufacutred by Leslie T. Miller of Baltimore, Maryland. The power to the unit was supplied by two 6-volt wet-cell lead-acid batteries. The bias D.C. voltage was maintained by a transistorized A.C.-D.C. transformer. An EICO Model 377 wave-generator and a Dumont Model 304-A oscilloscope were employed for anemometer adjustments. The outputs were recorded on two Hewlett-Packard X-Y recorders: the D.C. voltage output was directly fed into the Y-side of one of the recorders and the fluctuating part into the same side of another through a Hewlett-Packard R.M.S. voltmeter.

Hot-wire probes are seen in Fig. 5: the straight-wire and slanted-wire probes are for velocity and turbulence measurements respectively. The wires are 0.00015 inch diameter tungsten, copper-plated everywhere except in the central sensing portion and soldered on to needles spaced about 1/8 inch apart; the mounted wire resistence, measured by a micro-ohm-meter, ranged from 6 to 12 ohms. The calibration of this unit has shown that the output may be considered linear with $\pm$ 3% accuracy.

Fig. 4 shows traversing mechanisms with probes in position; on the right, a helipot is also seen: its output is monitored into the X-side of the afore-mentioned two recorders to represent a length scale.

C. Experimental Procedure

The porous, metallic, outer cylinder was left untouched since only the zero-pressure-gradient case was considered. Before the experiments were begun, the Plexiglas cylinder was smoothed with a rubbing compound, and a boundary-layer trip of one-inch-wide sand-paper band was placed on it two feet before the beginning of the test section.

The first measurements were of the wall shear stress, the velocity profile, and the turbulent-shear-stress profile at various stations without any roughness element. After it was confirmed that the boundary layer possessed fully-developed velocity and shear-stress characteristics a roughness fence was placed at $x = 6.25$ inches, the origin of x-co-ordinate being the beginning of the test channel.

For the wall-shear-stress measurements, the Preston tube was placed beside a static-pressure tap, and the pressure difference between

the two was read directly on the micromanometer in units of millimeter-methanol.

Since the time-mean velocity and velocity-fluctuation measurements required a different hot-wire probe from that used for the turbulent shear stress, the former was completed before the latter for each protuberance. When the straight-wire probe was installed in the traversing mechanism, care was taken to align it to the direction of the maximum D.C. voltage output. In case of the slanted-wire shear-stress probe, the alignment was such that the D.C. voltage output would not change appreciably when the direction of the wire was turned 90° in the vicinity of the wall.

D. Data Reduction

Data reduction was carried out with three computer programs run on the electronic digital computer of the M.I.T. Mechanical Engineering Department - IBM 1130 system. The first program evaluated the wall shear stress according to the Patel correlation [Ref. 16]:

$$\begin{aligned} 2.9 \geq x^* \geq 0.0 \qquad & y^* = 0.5x^* + 0.037 \\ 5.6 \geq x^* \geq 2.9 \qquad & y^* = 0.8287 - 0.1381\, x^* + 0.1437\, x^{*2} - 0.0060\, x^{*3} \\ x^* \geq 5.6 \qquad & x^* = y^* + 2.0 \log (1.95\, y^* + 4.10) \end{aligned} \tag{11}$$

where $x^* \equiv \log (\Delta P_p d^2/4\rho\nu^2)$

$y^* \equiv \log (u_*^2 d^2/4\rho\nu^2)$

The second program calculated time-mean velocities, velocity fluctuations, displacement thicknesses, momentum thicknesses and shape factors. The axi-symmetric definitions of the integral quantities were

used: the integrands in the Cartesian coordinate system were multiplied by a correction factor (1 + y/R). The numerical integration was performed with Simpson's rule.

The third program reduced the shear-stress data according to the following formula [Ref. 63].

$$-\overline{u'v'} = \frac{1}{4} U_\infty W_k \tan \alpha \left[(\overline{c_1^2}/C_1^2) - (\overline{c_2^2}/C_2^2) \right] \qquad (12)$$

where $\overline{c^2} \equiv$ the fluctuating voltage output squared

$C \equiv$ the D.C. voltage output

$W_k \equiv - \frac{0.3467}{\ell n \, (C_{\pi/4}/C_{\pi/2})}$: wire constant

$\alpha \equiv$ the angle between the shear-stress wire and the flow direction

The subscripts 1 & 2 indicate two orientations of the slanted wire.

E. Accuracy

As noted above, the uncertainty in the pressure measurements with the micromanometer was 5.75×10^{-6} psi; in case of the Preston tube measurements, this corresponded to the maximum of 1% error in ΔP. The calculated skin friction coefficients within 30 roughness-heights downstream of the protuberances, however, cannot be trusted to any degree because of the non-validity of the law of the wall in this region, on which the function of the Preston tube and the Patel correlations critically depend.

The hot-wire anemometer measurements were susceptible to such problems as non-linearity in the electronic equipment and probe mis-

orientation. Calibration of the electronic instruments after each boundary-layer traverse and careful alignment of the probes minimized the error. The slanted shear-stress-wire was aligned at the wall with some sacrifice of accuracy in the outer part of the boundary layer. With these precautions, the estimated errors are approximately 5 and 15% for velocity and turbulent-shear-stress measurements respectively. This estimate applies only to those regions where the ratio of velocity fluctuation to time-average velocity did not exceed 30%, and no wall effect was considered. An analysis of shear-stress errors due to misalignment of the slanted-wire probe is given by P. Goldberg [Ref. 13].

III. DISCUSSION

A. Wall Shear Stress

The experimental data are presented in Fig. 7. The skin-friction coefficients, C_f, were evaluated with the free-stream velocity at the entrance to the test channel. The measurements in the non-disturbed boundary layer show a gradual decrease along the test-section, which agrees with P. Goldberg's observation [Ref. 13]. The measurements after protuberances show a unique pattern of development: initially the value increases rapidly, presumably from zero, then it exceeds the values for the equilibrium boundary layer, and returns asymptotically to the equilibrium value from above; the whole response is similar to a critically damped oscillation of a dynamic system. The same phenomenon is reported by H. Ludwieg & W. Tillmann [Ref. 15].

From these observations, Schlichting's comment [Ref. 11] regarding a surface-roughness-transition problem, "... the shearing stress at the wall assumes its new value which corresponds to fully-developed flow immediately behind the two sections ...", appears to be in error, and this argument is supported by various recent investigators as stated by H. A. Panofsky & A. A. Townsend [Ref. 38].

The Ludwieg and Tillmann correlation of skin friction,

$$C_f = 0.0334/(\log R_\theta)^{1.838} \qquad (13)$$

failed to predict, not unexpectedly, the skin-friction coefficient in the transient region; since the law of the wall was found to be invalid in this region, the accuracy of Patel's calibration equations, Eq. (11), and the function of the Preston tube itself are in doubt.

Fig. 7 [II] shows the skin-friction-coefficients variation with a non-dimensionalized, spacial coordinate. All the points, except those associated with the smallest protuberance, appear to form a single curve, but this observation is questionable as evidenced by the exceptional group; the confirmation of this correlation has to wait for a more precise method of measuring the wall shear stress.

F. H. Clauser [Ref. 22] suggested a graphical method of obtaining wall shear stress from a velocity profile, utilizing the law of the wall: the rearrangement of Eq. (4) results in

$$\frac{\bar{u}}{U_\infty} = \sqrt{\frac{C_f}{2}} \left[\frac{1}{k} \ell n \left(\frac{yU_\infty}{\nu} \right) + \frac{1}{k} \ell n \left(\sqrt{\frac{C_f}{2}} \right) + A \right] \qquad (14)$$

Hence, the plot of $\bar{u}/U_\infty$ vs yU_∞/ν is unique for a given skin-friction coefficient whenever the law of the wall is valid. Several velocity profiles were plotted in this manner in Fig. 8. From these profiles, one can observe that, as far as the velocity profile is concerned, the effect is confined to a certain inner region for a small enough disturbance, and the unaffected outer region retains the original characteristics; on the other hand, the disturbed region is far from the fully-developed logarithmic profile, yet the existence of semi-logarithmically linear part in the velocity profile suggests a local equilibrium and the predominance of the local wall shear stress in this region.

B. Turbulent Shear Stress: $-\overline{u'v'}$

The turbulent-shear-stress data non-dimensionalized by the square of the free-stream velocity at the entrance to the test channel are presented in Fig. 9. Because of the finite dimension of the slanted-

wire shear-stress probe, no measurements were possible below y = 0.085 inches.

Equilibrium boundary layers showed approximately linear distributions as expected, but others demonstrated the distortion due to the roughness disturbance. Wherever the protuberance effect was felt, a distinct increase in turbulent shear stress was observed, and the distributions contain the maximum shear-stress points, the y-coordinate of which moves outward as in the case of a separating flow or a turbulent boundary layer in an adverse pressure gradient [see,for example, Ref. 12]. Fig. 9 [II] shows that the shear-stress profile has not recovered from the protuberance effect even at x = 31.0; from Fig. 13 [II] and Fig. 14 [II], the velocity profile may be considered to have regained the equilibrium profile by this point; this observation clearly exhibits the independence of velocity-profile development from that of the shear-stress profile, reflecting the importance of upstream history in turbulent-boundary-layer studies. The comparison of Fig. 9 [II] with Fig. 14 [II] also demonstrates the difference in the extent the roughness presence has been felt by the boundary layer: at x = 7.6, only 50% of the shear-stress profile appear to have been influenced, whereas at the same station, 90% of the velocity profile apparently have experienced the roughness presence. The response of shear stress lags, in general, behind that of time-average velocity. As the roughness height decreases, its effect on the velocity profile becomes confined to a certain inner region of the boundary layer, but the disturbance on the shear stress profile manages to propagate through the whole layer.

C. Velocity

The experimental time-mean velocity profiles and axial-velocity-fluctuation profiles are presented in Fig. 13 through Fig. 15: Fig. 13 magnifies the wall region, and Fig. 14 the outer wake region. The undisturbed reference profiles exhibit the equilibrium-boundary-layer characteristics, conforming to the universal similarity laws; others show definite deviations from them, although no observable effect appears in the defect law profile in the smallest protuberance case - the indication of the confined disturbance penetration.

A physical insight into the effects of roughness distrubances on the velocity profiles may be obtained from the Clauser plot of Fig. 8; these graphs do not contain the wall shear stress, and consequently, the uncertainty associated with it is eliminated. As mentioned before, the curves indicate that the layer close to the wall rapidly adjusts itself to local conditions. The disturbed portion of the profile is dominated by the local wall shear stress and the "y-coordinate" of the logarithmic region appears to move outward. In Fig. 8 [IV], the profile at $x = 6.8$ ($\frac{x-x_0}{h} = 17.2$) does not possess a logarithmic part. The reason, probably, is that the disturbance effect has just "swallowed" all of the original logarithmic region at that location; the profile at $x = 7.5$ ($\frac{x-x_0}{h} = 43.1$) shows its reappearance. This plot also demonstrates the predominance of the original wall shear stress in the undisturbed region.

The examination of these plots shows that a clearly observable logarithmic region with a distinguishable buffer layer reappears approximately 30 roughness-heights downstream of the protuberance.

A speculation, conjectured from these observations, is that the undisturbed outer region of the velocity profile is the remnant of the original equilibrium layer which existed upstream of the protuberance, and the wall layer of the disturbed inner region is in local equilibrium at least for $\frac{x-x_0}{h} \geq 30$. This thought appears to confirm the two-layer model used by Elliot [Ref. 36] and Panofsky & Townsend [Ref. 38]. Their shortcoming, however, enters when the internal boundary layer is assumed to be in a fully-developed form; on the contrary, the dominating factor, the wall shear stress, is a strong function of the streamwise coordinate. Furthermore, this confirmation applies only to those roughnesses with height smaller than about 8% of the undisturbed, original, boundary-layer thickness. For larger roughnesses, the disturbance caused is strong enough to affect the whole layer before the reappearance of the logarithmic region, and the two-layer model becomes invalid.

Velocity fluctuations were normalized by the local time-average velocity and are presented in Fig. 15. A conspicuous trend is their rapid recovery from the disturbance, and the recovery distance appears to correspond to that of the shape factor noted below. The reliability of the hot-wire anemometer measurements is known to hold for the normalized velocity fluctuation less than 30%; hence, according to Fig. 15, some of the velocity measurements have to be deemed doubtful, especially in the wall region.

Integrated parameters and their ratio, δ^*, θ, and H, were normalized by their respective non-perturbed values at x = 6.25 and were plotted against the non-dimensionalized streamwise coordinate as shown in Fig. 10 through Fig. 12. These reference data,

$\delta_0^* = 0.0936$ inches

$\theta_0 = 0.0652$ inches

$H_0 = 1.435$

were taken on one day and were used for all the calculations. The dotted lines are the experimentally determined development of the unperturbed boundary-layer values.

A notable observation here is the concentrated appearance of roughness effect in the vicinity of the roughness element as well as its non-appearance for the three smallest protuberances. The rapid recovery of the shape factor within 100 roughness-heights is also noteworthy. All the integrated parameters apparently return to the original non-perturbed values far downstream of the protuberance and no significant influence of the perturbations is detectable; this simply means that the disturbance effects become immeasurably small, though they still do exist.

IV. CONCLUSIONS

The experimental investigation of the response of an incompressible, fully-developed, equilibrium turbulent boundary layer to a two-dimensional perturbation lead to the following conclusions.

1) The effect of the perturbation can be confined to a certain portion of the boundary layer if it is small enough, and the appreciable changes in integral quantities, δ^* and θ, are observable only in the vicinity of its occurrence - within 250 roughness-heights. Their ratio, H, returns to the initial value much earlier - within 100 roughness-heights.

2) The wall shear stress, the turbulent shear stress, the time-mean velocity and the velocity fluctuation show independent responses and undergo individual developments, reflecting the importance of past history in the study of turbulent boundary layers.

3) The wall shear stress displays a unique and rapid development in the region close to the protuberance, returning to the fully-developed value within 150 roughness-heights. An empirical correlation of the development with x and h appears to be possible, but the uncertainty involved in its determination prevents its universal validity. This uncertainty on the other hand stresses the urgent need for an accurate method of wall-shear-stress determination not only for this study but also for the general interest.

4) The linear equilibrium profile of turbulent shear stress becomes distorted by the disturbance, and the disturbed boundary layers exhibit a temporary and partial increase in value and a maximum like a turbulent boundary layer in an adverse pressure gradient. The y-coordinate of the

maximum shear point propagates outwards with the streamwise distance.

5) The disturbed velocity profiles demonstrate a self-preserving feature at least in form. In the wall region, the profiles quickly adjust themselves to the local conditions, evidenced by the appearance of a logarithmic profile after approximately 30 roughness-heights downstream of the point of the disturbance occurrence. For a small enough disturbance, $h/\delta_0 \leq 0.08$, the governing parameter in the inner region is the local wall shear stress, whereas in the outer region, it is the original wall shear stress of the boundary layer before encountering the protuberance. This fact justifies the concept of "internal boundary layer" and the two-layer model used for the roughness transition problem by several investigators. The velocity profile in the internal boundary layer is in local equilibrium for $(x-x_0/h \geq 30$, but it is far from the fully-developed one.

V. RECOMMENDATIONS FOR FURTHER WORK

A. Thoughts on the Theoretical Approach

From this investigation, a possible analytical approach to the problem was conceived, but due to the uncertainty involved in the skin-friction determination, the analysis leaves much to be desired. Consequently, only an outline is presented here solely to provoke further thought.

As stated before, the two-layer model used for the roughness transition problems by Elliot [Ref. 36] and Panofsky & Townsend [Ref. 38], appears to be valid in the present case of an equilibrium boundary layer perturbed by a two-dimensional protuberance; furthermore, the wall shear stress, which existed before any part of the boundarylayer had felt the presence of the roughness element, retains its predominance over the undisturbed part of the boundary layer. Only one serious criticism to be made for their analyses is the assumption of the fully-developed wall shear stress immediately after the occurrence of the perturbation. Since the appreciable influence of the disturbance is detectable only in the vicinity of its incidence, where the wall shear stress itself is undergoing a rapid change, no analysis can ignore this variation.

The analytical method suggested is the "parametric integral method" [see Ref. 43, 44, and 45]: a boundary layer is split into two parts, the internal boundary layer and the outer layer, and the integral-momentum equation is applied to each part. The assumed velocity profile for the internal boundary layer is the modified law of the wake with local parameters and the one for the outer layer is the law of the wake with the parameters of the initial undisturbed boundary layer. Since

this method requires the knowledge of shear stress at the junction of the two layers, the shear-stress-velocity-gradient relationship for the fully-turbulent and equilibrium part of the turbulent boundary layer, derived from the turbulent energy equation by A. A. Townsend [Ref. 28], may be used; its applicability may be questioned, but, since the boundary layer concerned is an equilibrium one and the outer region is undisturbed, the use is probably justified.

There are four unknowns associated with the internal boundary layer - δ_{in}, u_*, v_*, and $\bar{v}$. Empirical approximations to the variation of u_* with x and h, shown in Fig. 7, can be used. Therefore, the three equations stated above can be integrated and rearranged to form three first-order ordinary differential equations of δ_{in}, v_*, and $\bar{v}$ with x as the sole independent variable. These equations can be integrated further by any one of the numerical integration methods. This analysis actually resulted in one ordinary differential equation and two algebraic equations.

B. Extension to the Present Study

The urgent need for a reliable method of skin-friction determination is apparent. As long as empirical correlations are used in engineering analysis concerning viscous fluid (this, I believe, will be true for many years to come), the wall shear stress plays such an important part that it should be accurately determinable under any circumstances.

In actual turbomachinery, boundary layers are always subjected to pressure gradients, so a similar investigation to the present one should be performed in pressure gradients - possibly the ones typical of the

rotating machineries. Also from the practical point of view, the roughness should be made three-dimensional. Though the uncertainty involved in wall shear stress may prove to be prohibitive, some empirical or semi-empirical theory should be formulated with the ultimate objective of being able to predict everything before, during and after the perturbation, if all the information about the undisturbed state is known.

REFERENCES

1. Klebanoff, P.S. & Diehl, Z.W., "Some Features of Artificially Thickened Fully Developed Turbulent Boundary-Layers with Zero Pressure Gradient," NACA Report, No.1110, 1952

2. Pinkerton, R.M., "Calculated and Measured Pressure Distribution over the Mid-span Section of the NACA 4412 Airfoil," NACA Report, No.563, 1936

3. Preston, J.H. & Maskell, E.C. Quoted from Ref.5

4. Schneider, K.H., "Potential Flow Through a Cascade of Known Airfoils," M.I.T. Gas Turbine Lab. Report, No.32, 1955

5. Schneider, K.H., "Boundary Layer Effects on Airfoil Lift," M.I.T. Gas Turbine Lab. Report, No.47, 1958

6. Spence, D.A., "Prediction of the Characteristics of Two-Dimensional Airfoils," J. Aero. Sci., Vol.21, p.577, 1954

7. Theodorsen, T. & Garrick, I.E., "General Potential Theory of Arbitrary Wing Sections," NACA Report, No.452, 1933

8. Clauser, F.H., "The Turbulent Boundary Layer," Advances in Applied Mechanics, Vol.4, p.1, 1956

9. Coles, D., "The Law of the Wake in the Turbulent Boundary Layer," J. Fluid Mechanics, Vol.1, p.191, 1956

10. Rotta, J.C., "Turbulent Boundary Layers in Incompressible Flow," Progress in Aero. Sci., Vol.2, p.1, Pergamon Press, 1962

11. Schlichting, H., "Boundary Layer Theory," McGraw Hill Book Comp., Inc., 1960

12. Sovran, G., "Fluid Mechanics of Internal Flow," Elsevier Publishing Comp., 1967

13. Goldberg, P., "Upstream History and Apparent Stress in the Turbulent Boundary Layers," M.I.T. Gas Turbine Lab. Report, No.85, 1966

14. Kline, S.J. et al., "The Structure of Turbulent Boundary Layer," J. Fluid Mechanics, Vol.30, Part 4, p.741, 1967

15. Ludwieg, H. & Tillmann, W., "Investigation of the Wall Shearing Stress in Turbulent Boundary Layers," NACA Report, TM No.1285, 1950

16. Patel, V.C., "Calibration of the Preston Tube and Limitation on its Use in Pressure Gradient," J. Fluid Mechanics, Vol.23, P.185, 1965

17. Preston, J.H., "The Determination of Turbulent Skin Friction by Means of Pitot Tubes," J. Royal Aero. Soc., Vol.58, p.109, 1954

18. Hama, F.R., "On the Velocity Distribution in the Laminar Sublayer and Transition Region in Turbulent Shear Flow," J. Aero. Sci., Vol.20, p.648, 1953

19. Kleinstein, G., "Generalized Law of the Wall and Eddy-Viscosity Model for Wall Boundary Layer," AIAA J., Vol.5, No.8, p.1402, 1967

20. Spalding, D.B., "A Single Formula for the 'Law of the Wall'," ASME J. Applied Mechanics, Vol.28, p.455, 1961

21. Bradshaw, P., "The Turbulent Structure of Equilibrium Boundary Layers," J. Fluid Mechanics, Vol.29, p.625, 1967

22. Clauser, F.H., "Boundary Layer in Adverse Pressure Gradients," J. Aero. Sci., Vol.21, p.91, 1954

23. Coles, D., "Remarks on the Equilibrium Turbulent Boundary Layer," J. Aero. Sci., Vol.24, p.495, 1957

24. Mellor, G.L., "Equilibrium Turbulent Boundary Layers," AIAA J., Vol.2, p.1650, 1964

25. Mellor, G.L., "The Effect of Pressure Gradients on Turbulent Flow near a Smooth Wall," J. Fluid Mechanics, Vol.24, p.255, 1966

26. Mellor, G.L. & Gibson, D.M., "Equilibrium Turbulent Boundary Layers," J. Fluid Mechanics, Vol.24, p.225, 1966

27. Townsend, A.A., "The Properties of Equilibrium Boundary Layers," J. Fluid Mechanics, Vol.1, p.561, 1956

28. Townsend, A.A., "Equilibrium Layers and Wall Turbulence," J. Fluid Mechanics, Vol.2, p.97, 1961

29. Townsend, A.A., "Self-preserving Flow inside a Turbulent Boundary layer," J. Fluid Mechanics, Vol.22, p.773, 1965

30. Hama, F.R., "Boundary Layer Characteristics for Smooth and Rough Surfaces," Transaction, Soc. Nav. Arch. Marin. Eng., Vol.62, p.333, 1954

31. Perry, A.E. & Joubert, P.N., "Rough-Wall Boundary Layers in Adverse Pressure Gradients," J. Fluid Mechanics, Vol.17, p.193, 1963

32. Tewfik, O.E., "Some Effect of Surface Roughness on the Turbulent Boundary Layer," AIAA J., Vol.1, p.2178, 1963

33. van Driest, E.R., "On Turbulent Flow Near a Wall," J. Aero. Sci., Vol.23, p.1007, 1956

34. Bradshaw, P. & Ferriss, D.H., "The Effect of Initial Conditions on the Development of Turbulent Boundary Layers," Defence Documentation Center Report, No.AD660621, 1967

35. Blackadar, A.K. et al., "Determination of the Effect of Roughness Change on the Wind Profile," Physics of Fluids, Vol.10, No.9, Part.2, p.S209, 1967

36. Elliott, W.P., "The Growth of the Atmospheric Internal Boundary Layer," Transaction, American Geographical Union, Vol.39, p.1048, 1958

37. Jacobs, W., "Umformung eines turbulenten Geschwindigkeits-Profils," ZAMM, Vol.19, p.87, 1939

38. Panofsky, H.A. & Townsend, A.A., "Change of Terrain Roughness and the Wind Profile," Quart. J. Royal Meteor. Soc., Vol.90, p.147, 1964

39. Taylor, R.J., "Small Scale Advection and the Neutral Wind Profile," J. Fluid Mechanics, Vol.13, p.529, 1962

40. Townsend, A.A., "The Response of a Turbulent Boundary Layer to Abrupt Changes in Surface Conditions," J. Fluid Mechanics, Vol.22, p.799, 1965

41. Townsend, A.A., "The Flow in a Turbulent Boundary Layer after a Change in Surface Roughness," J. Fluid Mechanics, Vol.26, p.255, 1966

42. "Hot-wire Anemometer Manual," Flow Corporation, Watertown, Mass.

43. Launder, B.E., "Laminarization of the Turbulent Boundary Layer by Acceleration," M.I.T. Gas Turbine Lab. Report, No.77, 1964

44. Moses, H.L., "The Behaviour of Turbulent Boundary Layers in Adverse Pressure Gradients," M.I.T. Gas Turbine Lab. Report, No.73, 1964

45. Nash-Webber, J.L., "Wall Shear-Stress and Laminarization in Accelerated Turbulent Compressible Boundary Layer," M.I.T. Gas Turbine Lab. Report, No.94, 1968

TABLE [I]

h	$\frac{h}{\delta_0}$	$\frac{hu_{*0}}{\nu}$	$\frac{hU_\infty}{\nu}$	x	$x-x_0$	$\frac{x-x_0}{h}$	δ^*	θ	H	u_* !	τ_w !	C_f !
inch				inch	inch		inch	inch		$\frac{ft.}{sec.}$	psi $\times 10^6$	$\times 10^4$
				7.6	1.3	13.0	0.186	0.080	2.32	0.5011	3.96	2.3
0.100	0.148	96.2	2278.4	8.0	1.7	17.0	0.165	0.082	2.00	1.3940	30.67	17.9
				9.0	2.7	27.0	0.130	0.082	1.59	1.7259	47.00	27.5
				7.4	1.1	14.3	0.140	0.065	2.15	0.5565	5.11	3.0
0.077	0.124	74.1	1701.3	8.0	1.7	22.1	0.133	0.071	1.87	1.5086	37.56	22.0
				9.0	2.7	35.1	0.127	0.078	1.63	1.7661	51.47	30.2
				6.9	0.6	12.0	0.130	0.074	1.76	0.8902	11.69	6.8
0.050	0.081	48.1	1097.6	7.0	0.7	14.0	0.100	0.058	1.71	1.3736	27.83	16.3
				8.0	1.7	34.0	0.101	0.065	1.55	1.9107	53.86	31.4
				6.7	0.4	13.8	0.095	0.058	1.64	1.0948	19.19	11.2
0.029	0.048	27.9	684.2	6.8	0.5	17.2	0.098	0.062	1.59	1.3778	30.38	17.7
				7.5	0.7	24.1	0.099	0.063	1.58	1.9238	59.24	34.6

! Preston tube measurements

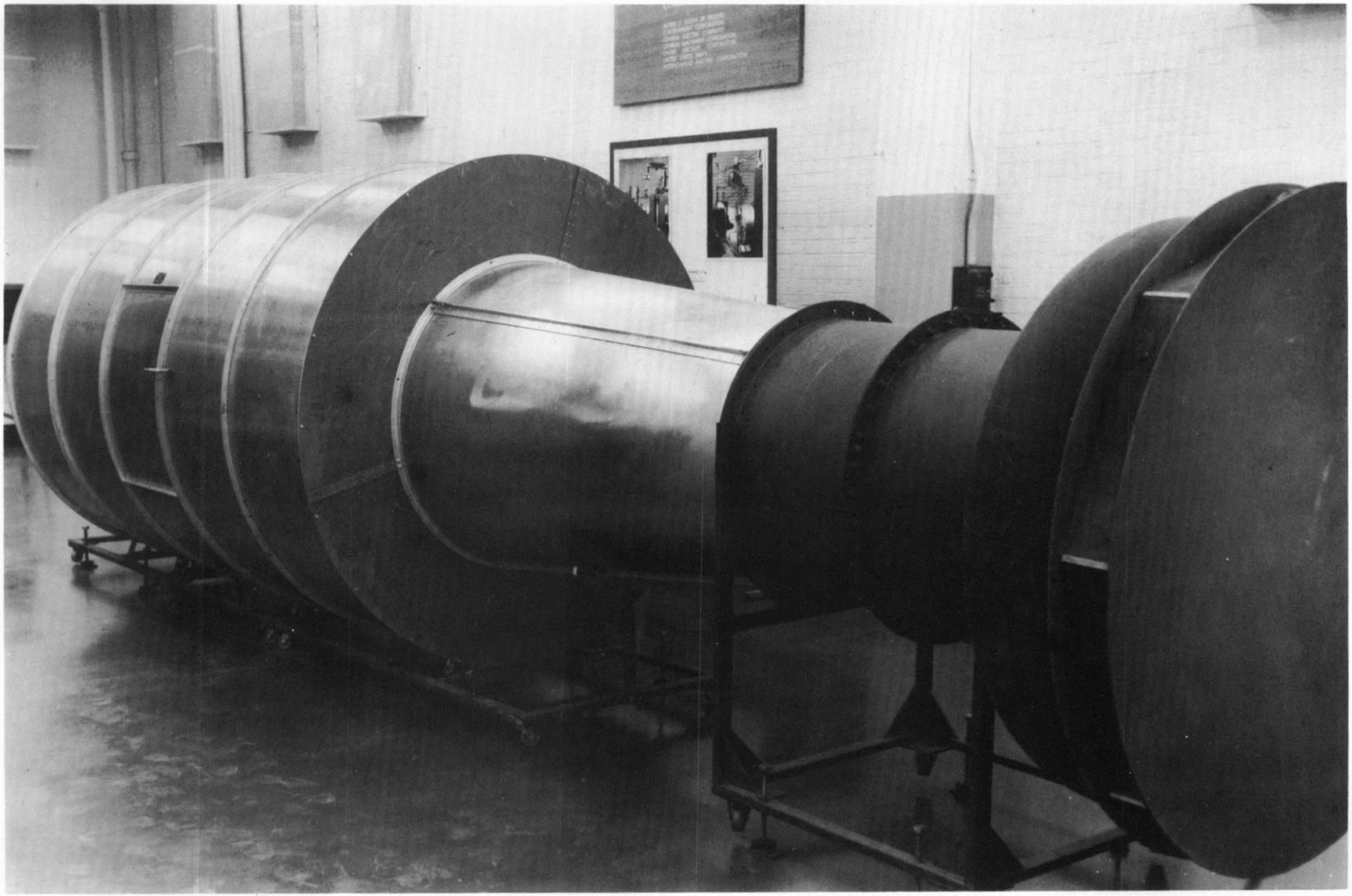

FIG.1 WIND TUNNEL

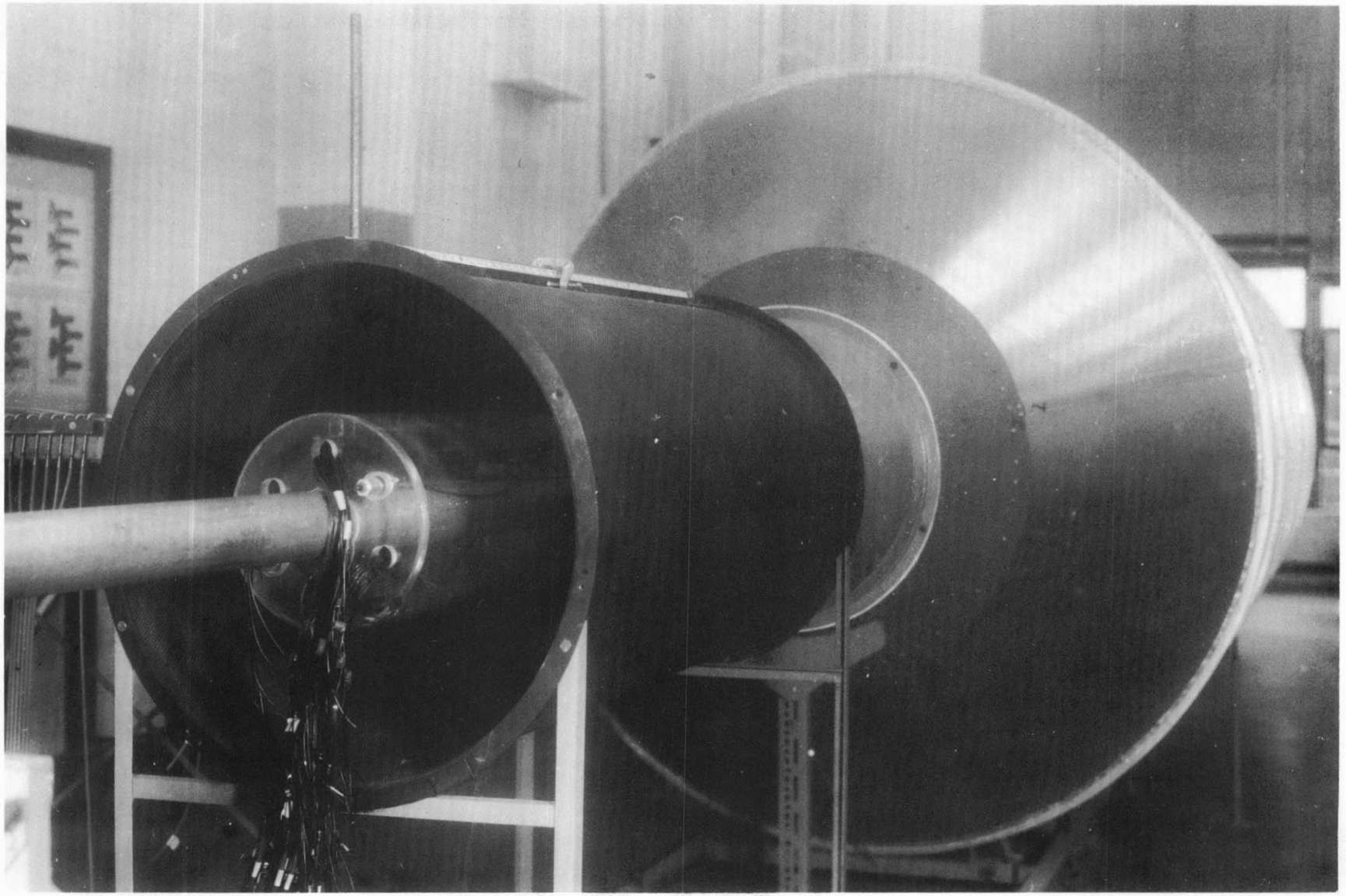

FIG.1 (Continued)

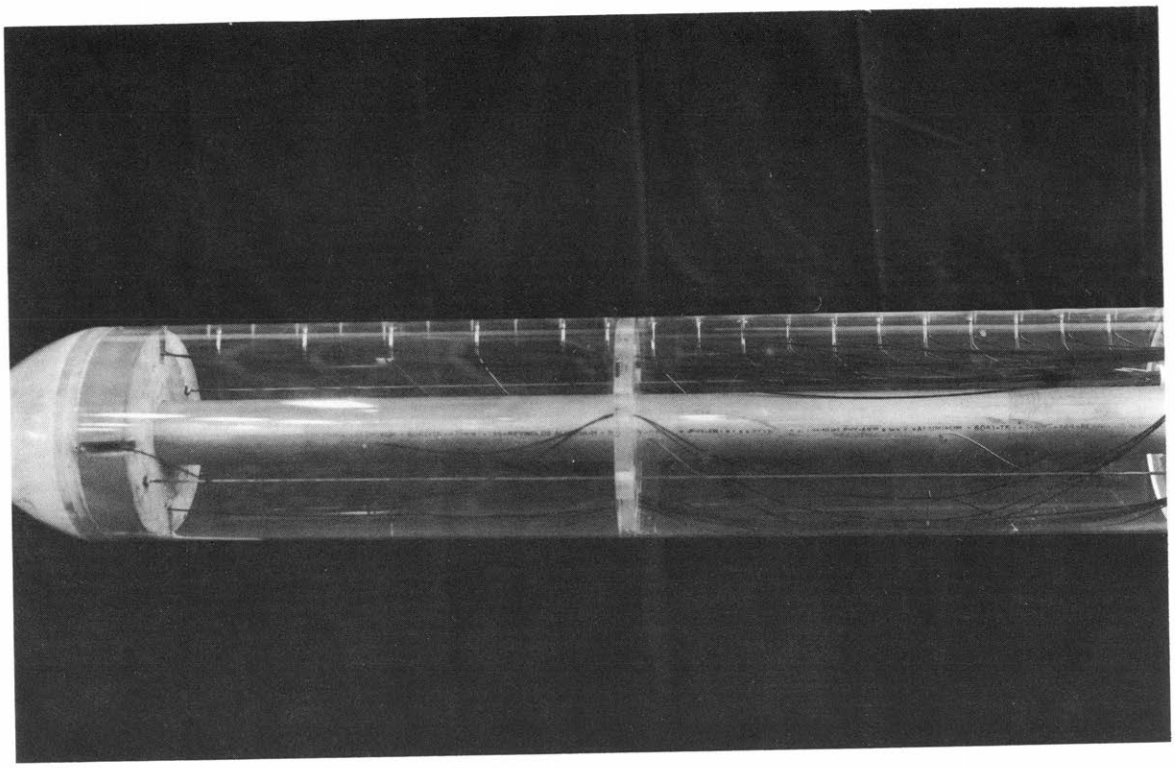

FIG.2 TEST CHANNEL INNER CYLINDER

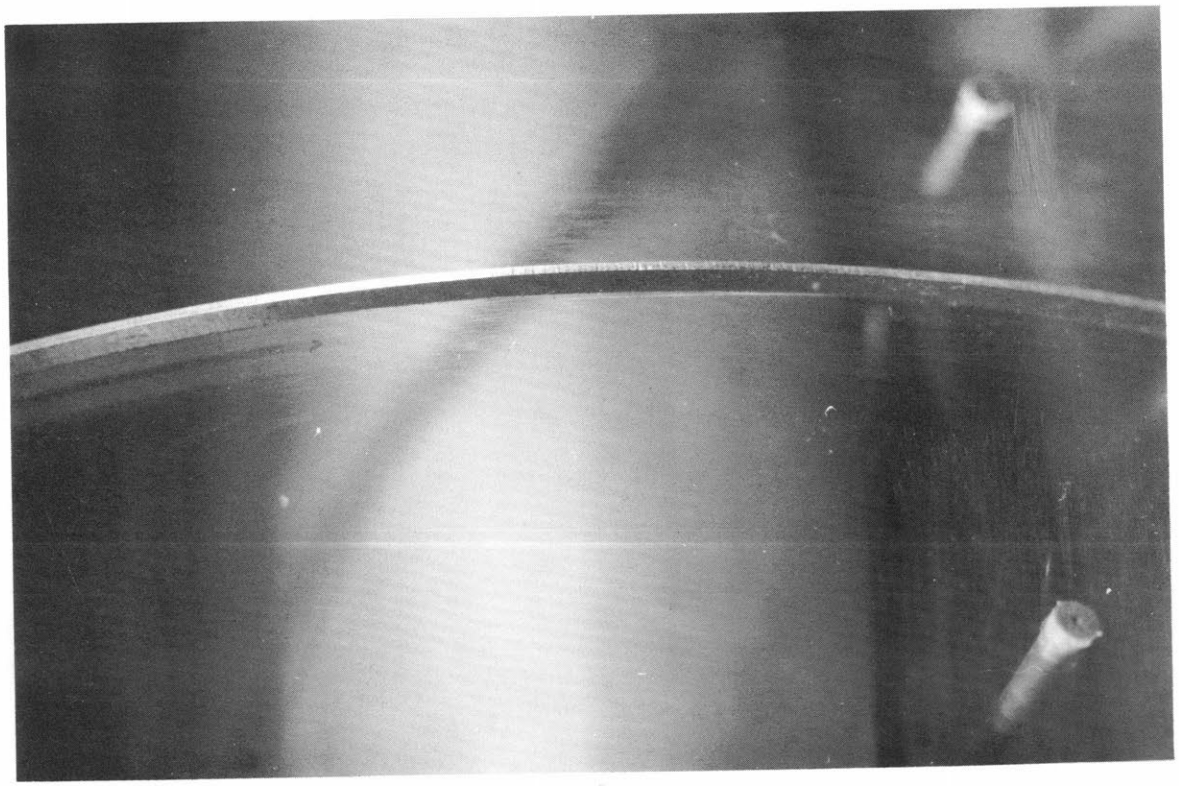

FIG.3 ROUGHNESS FENCE

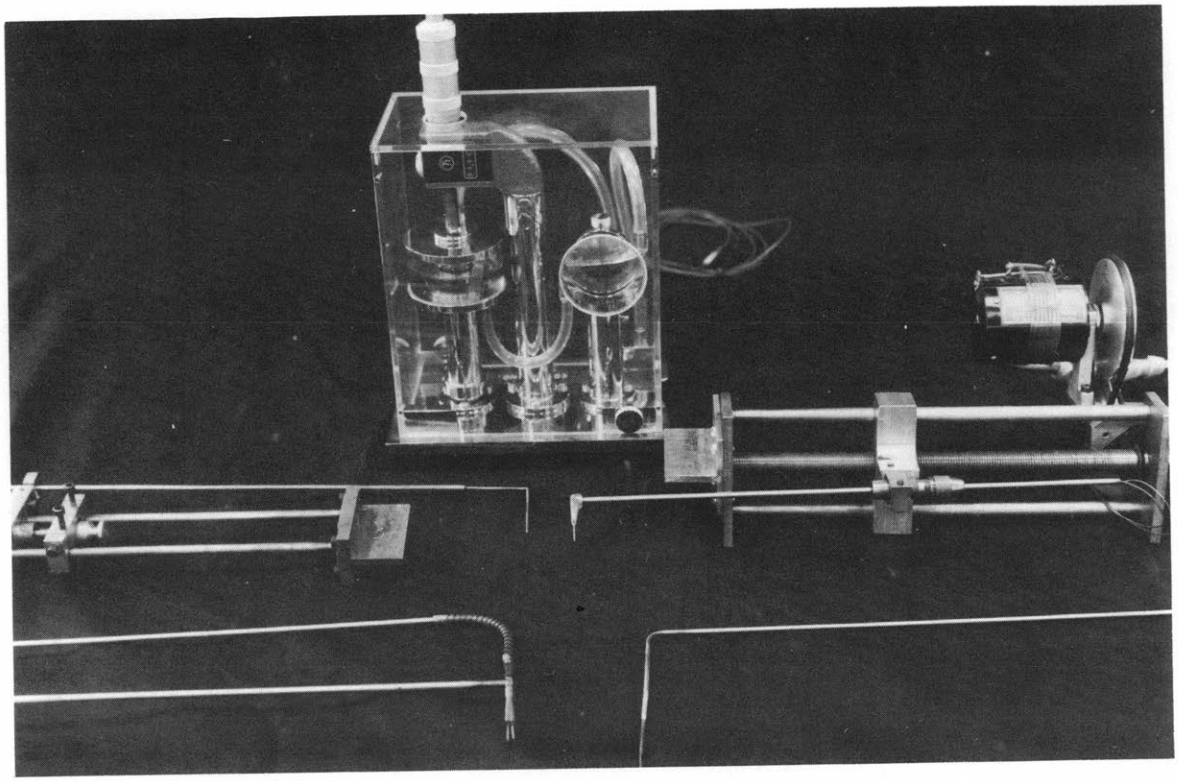

FIG.4 INSTRUMENTATION

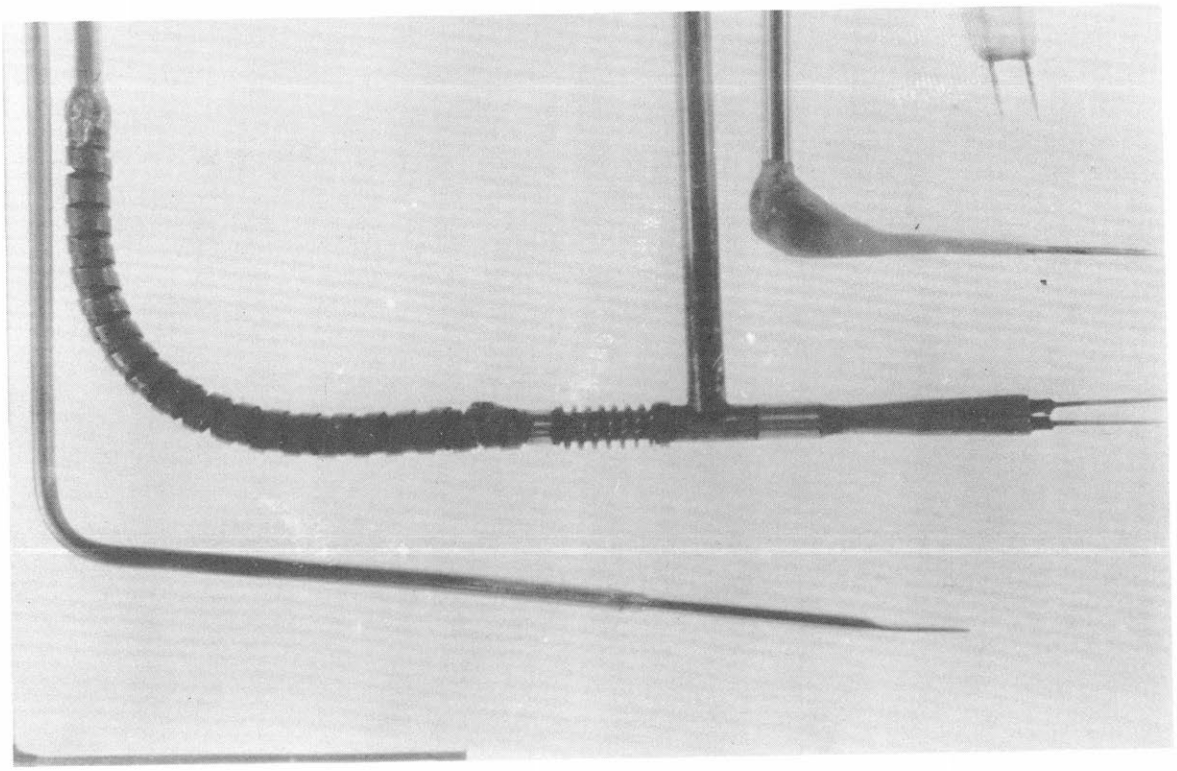

FIG.5 PROBES

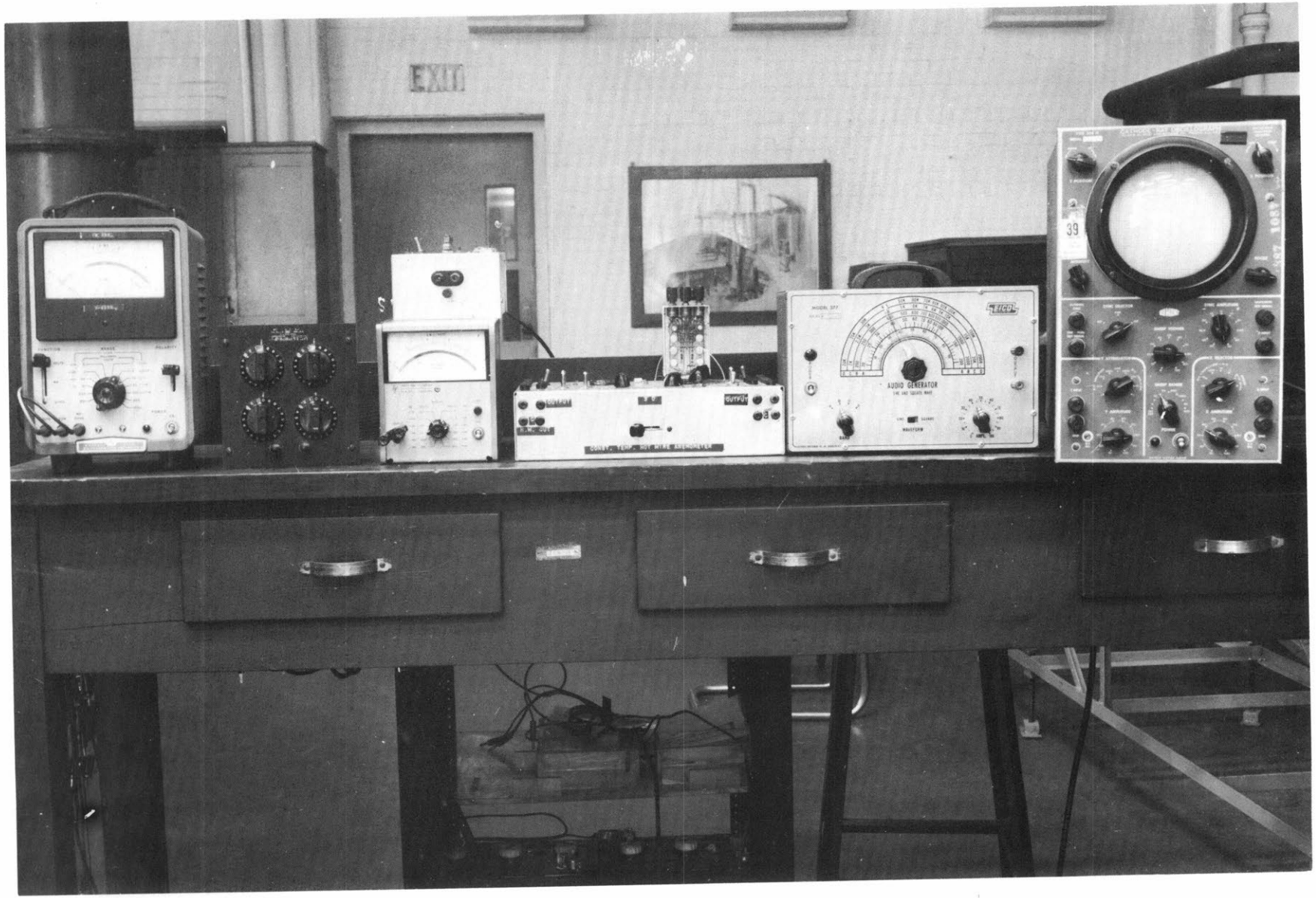

FIG.6 HOT-WIRE ANEMOMETER EQUIPMENT

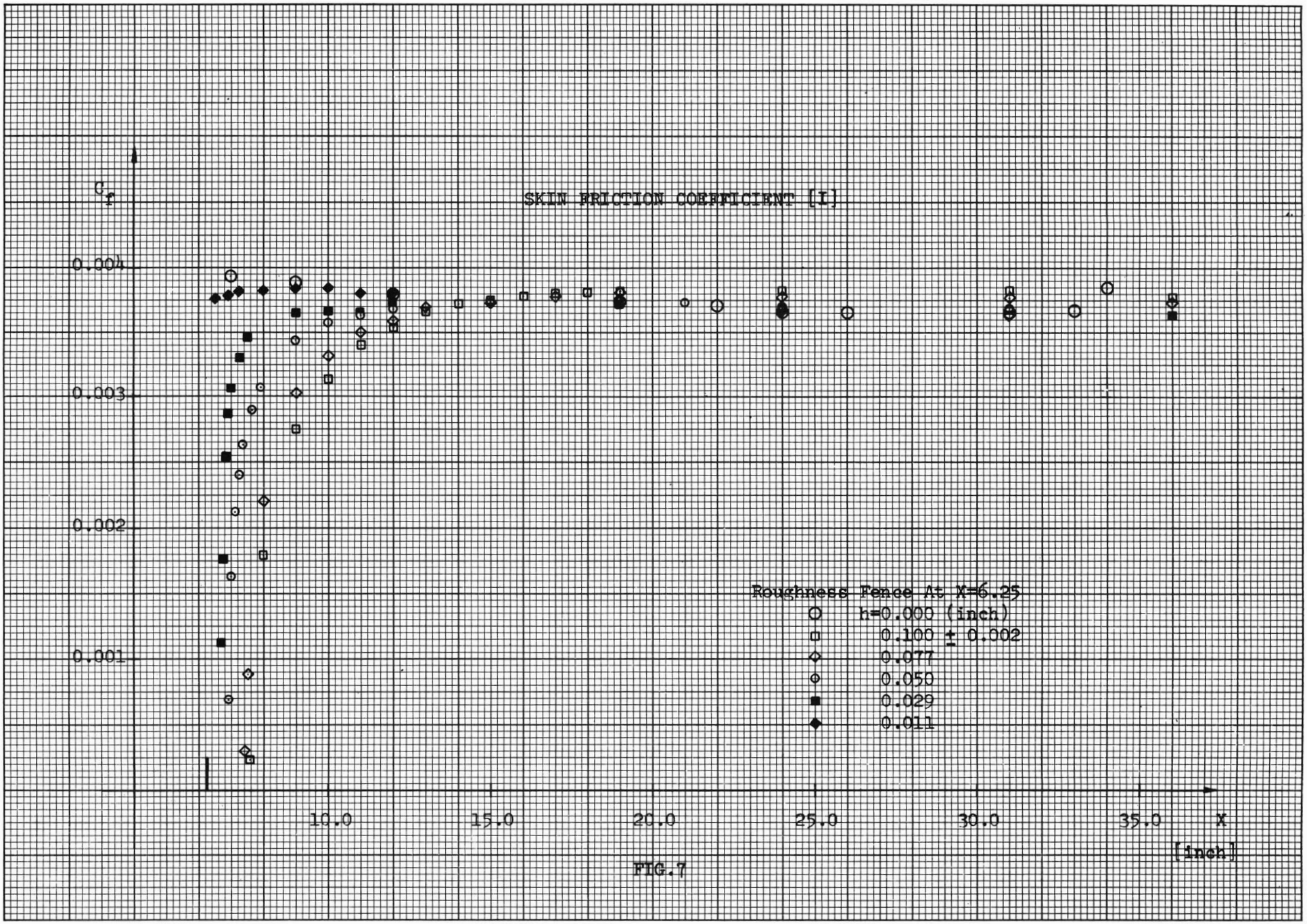
SKIN FRICTION COEFFICIENT [I]
C_f
0.004
0.003
0.002
0.001
Roughness Fence At X=6.25
h=0.000 (inch)
0.100 ± 0.002
0.077
0.050
0.029
0.011
10.0
15.0
20.0
25.0
30.0
35.0
X
[inch]

FIG.7

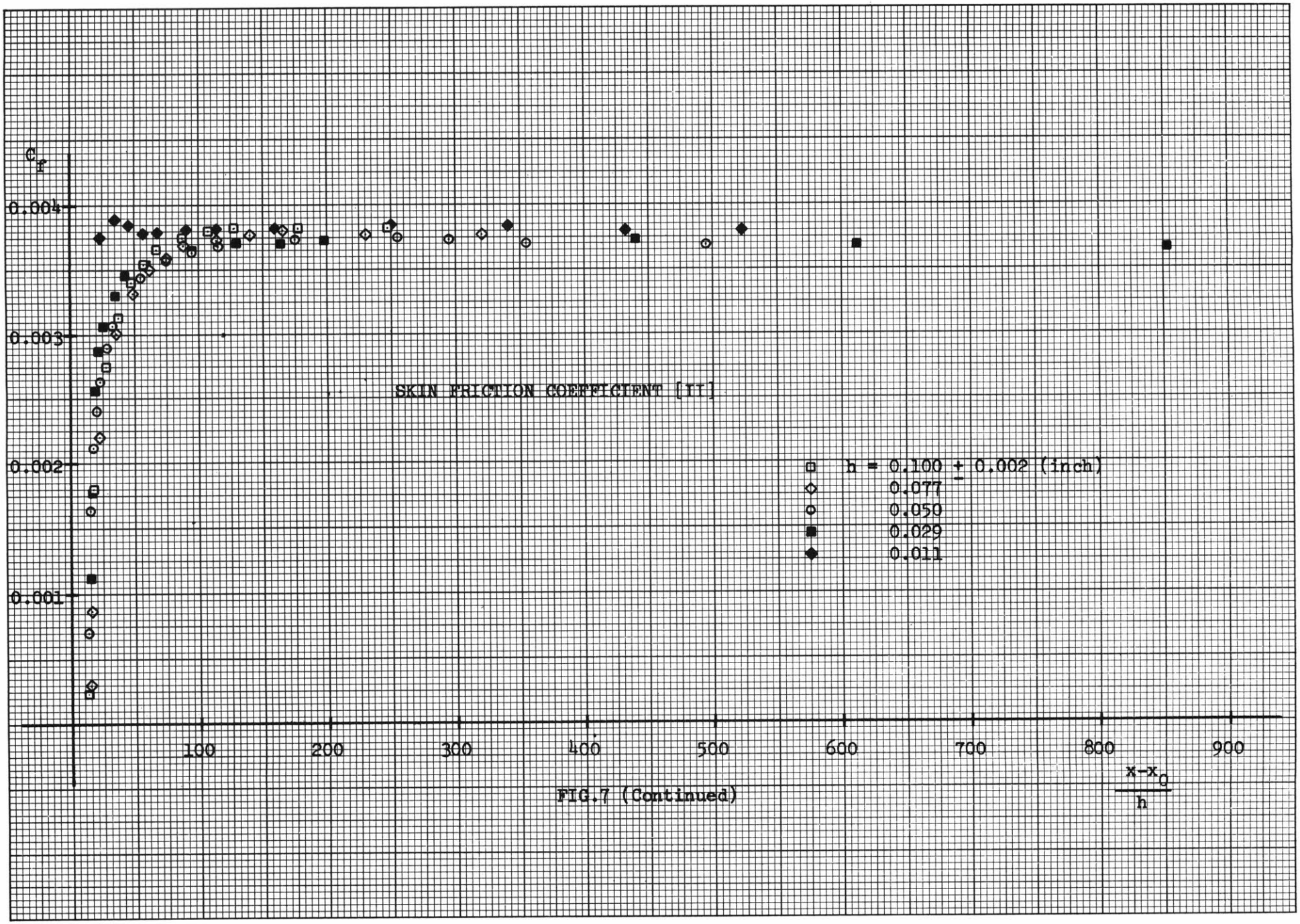

FIG.7 (Continued)

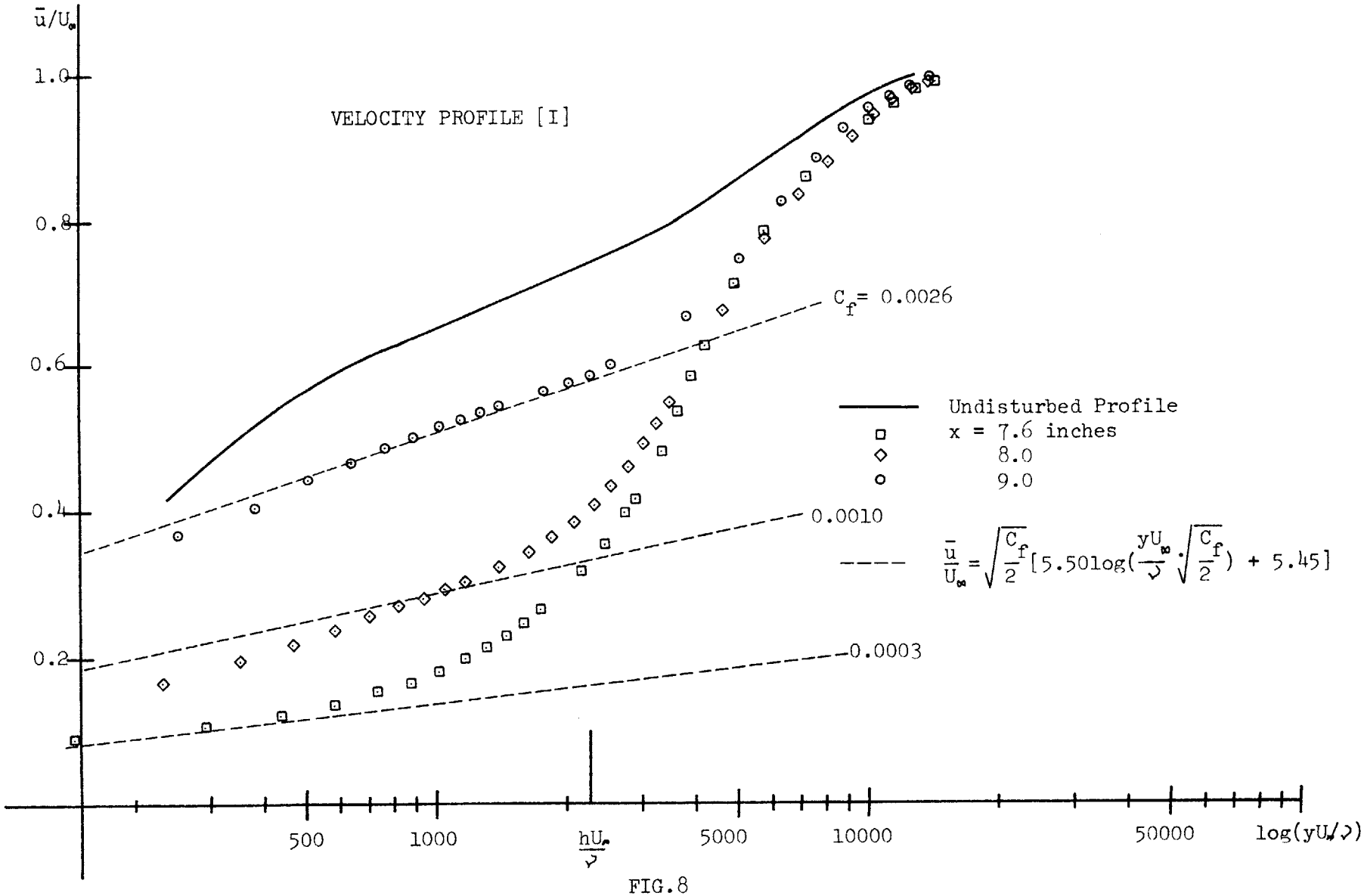
$\bar{u}/U_\infty$
1.0
0.8
0.6
0.4
0.2
VELOCITY PROFILE [I]
C_f= 0.0026
0.0010
0.0003
Undisturbed Profile
x = 7.6 inches
8.0
9.0
$\frac{\bar{u}}{U_\infty} = \sqrt{\frac{C_f}{2}}[5.50\log(\frac{yU_\infty}{\nu}\sqrt{\frac{C_f}{2}}) + 5.45]$
500
1000
$\frac{hU_\infty}{\nu}$
5000
10000
50000
$\log(yU_\infty/\nu)$

FIG.8

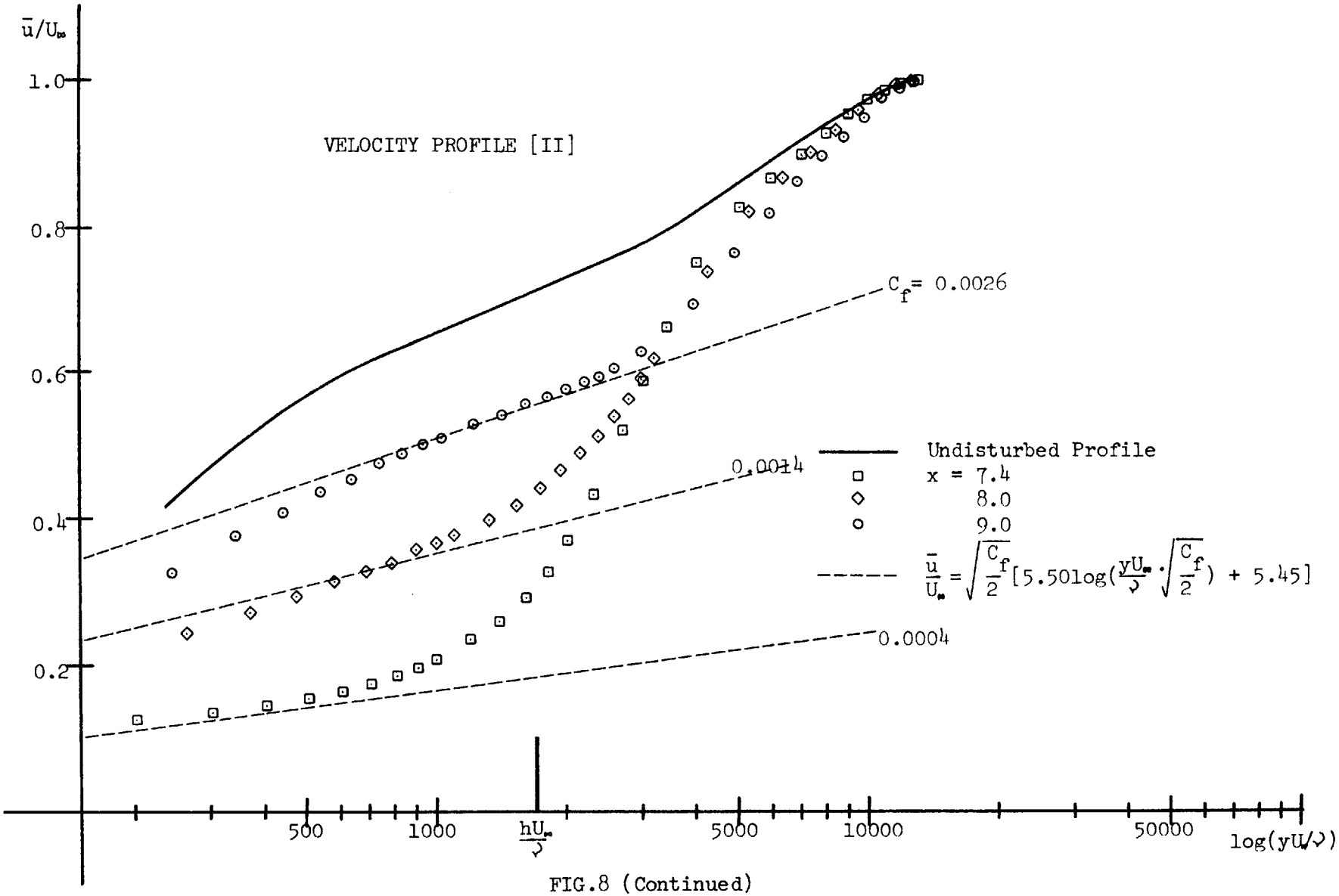

FIG.8 (Continued)

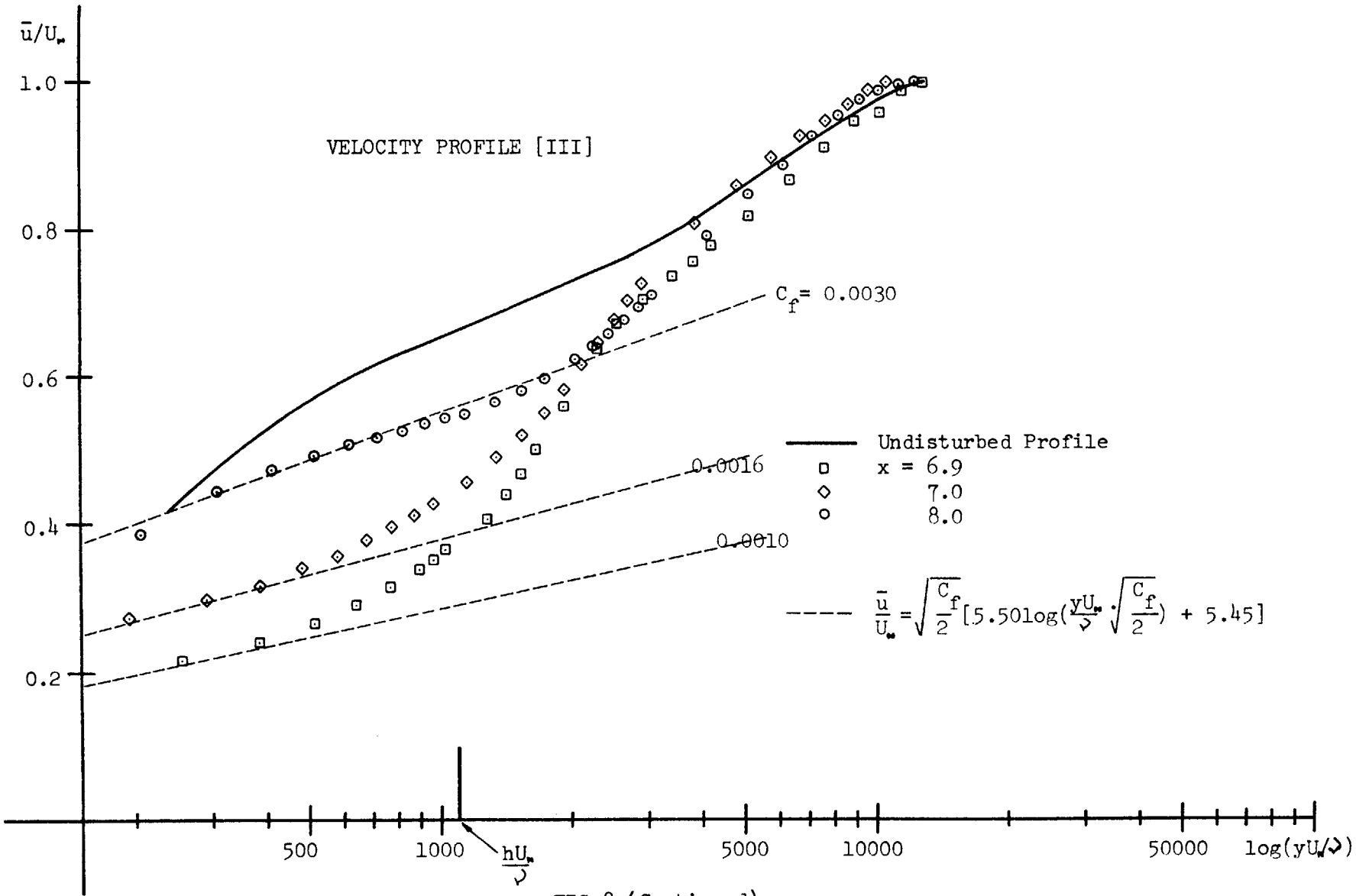

FIG.8 (Continued)

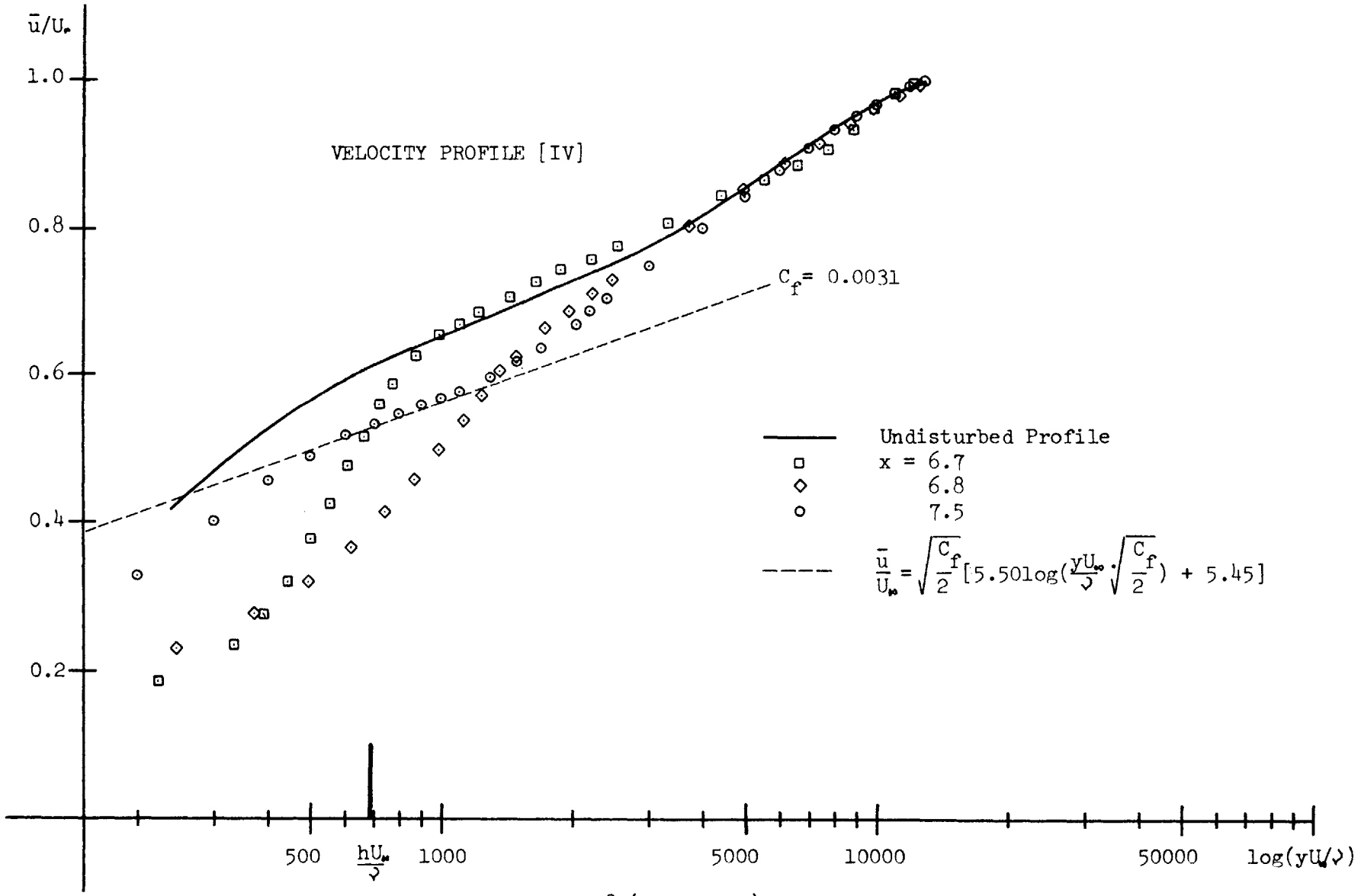

FIG.8 (Continued)

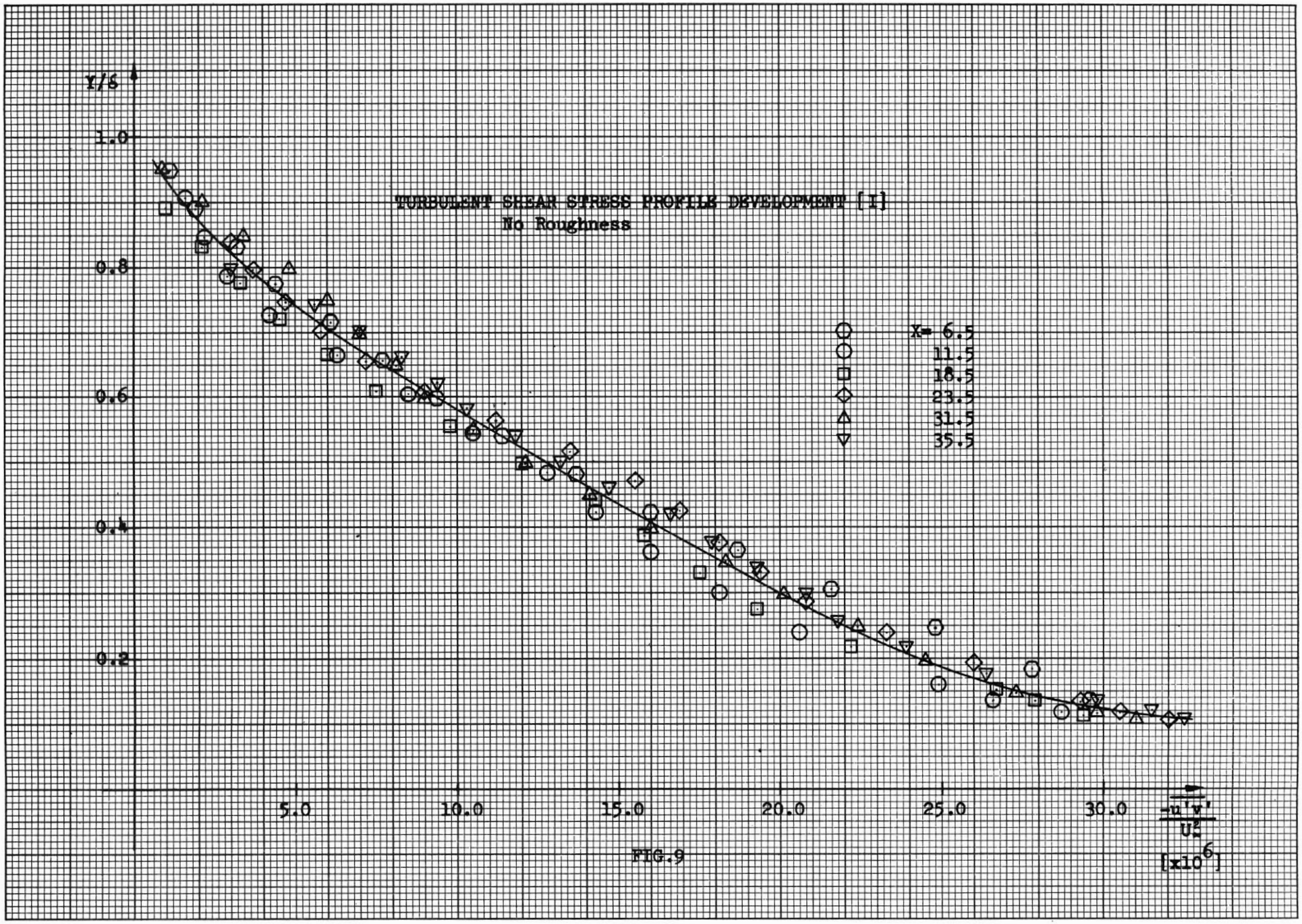
TURBULENT SHEAR STRESS PROFILE DEVELOPMENT [I]
No Roughness
Y/δ
1.0
0.8
0.6
0.4
0.2
X= 6.5
11.5
18.5
23.5
31.5
35.5
5.0
10.0
15.0
20.0
25.0
30.0
$\frac{-\overline{u'v'}}{U_e^2}$
[x10^6]

FIG.9

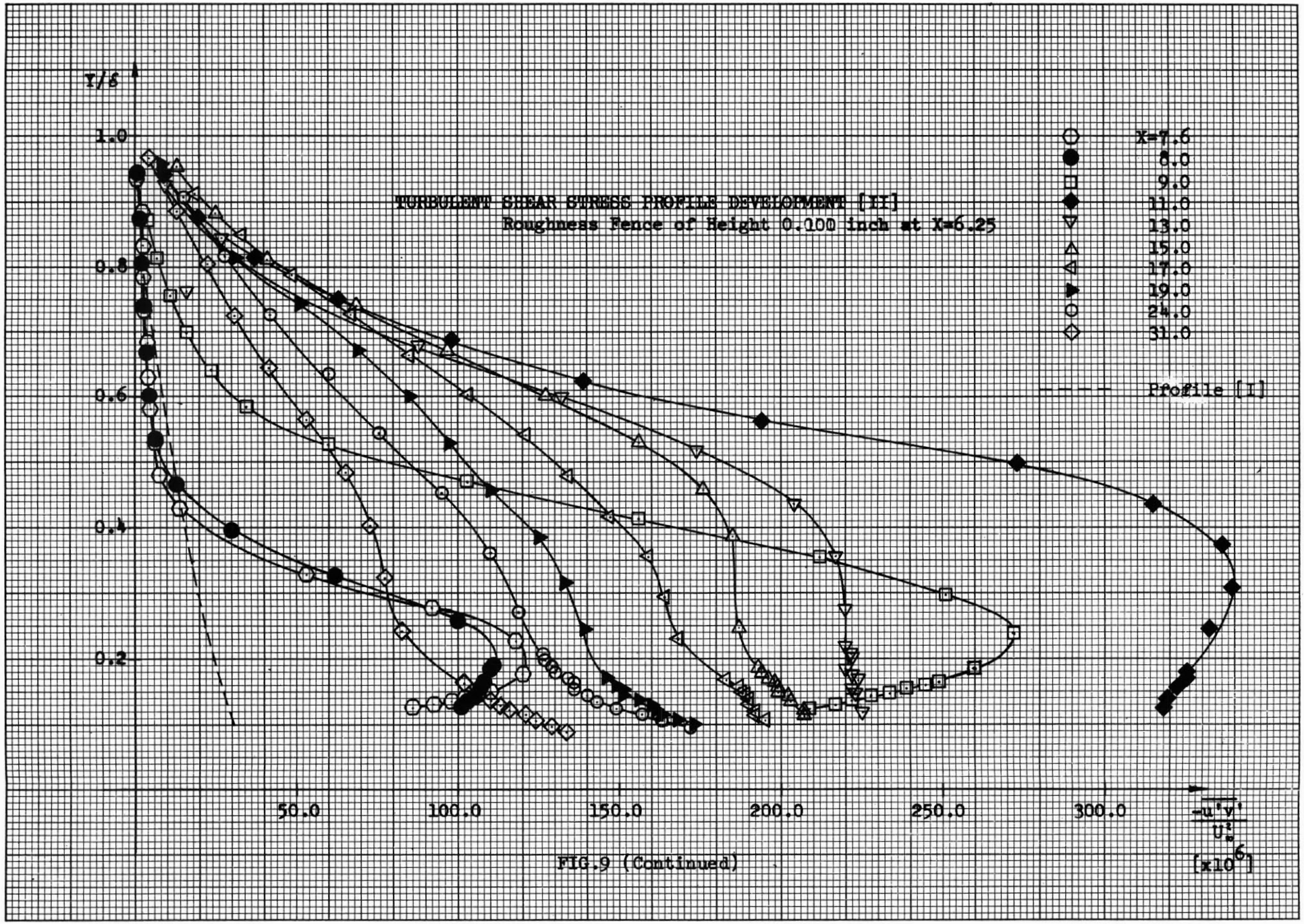

FIG.9 (Continued)

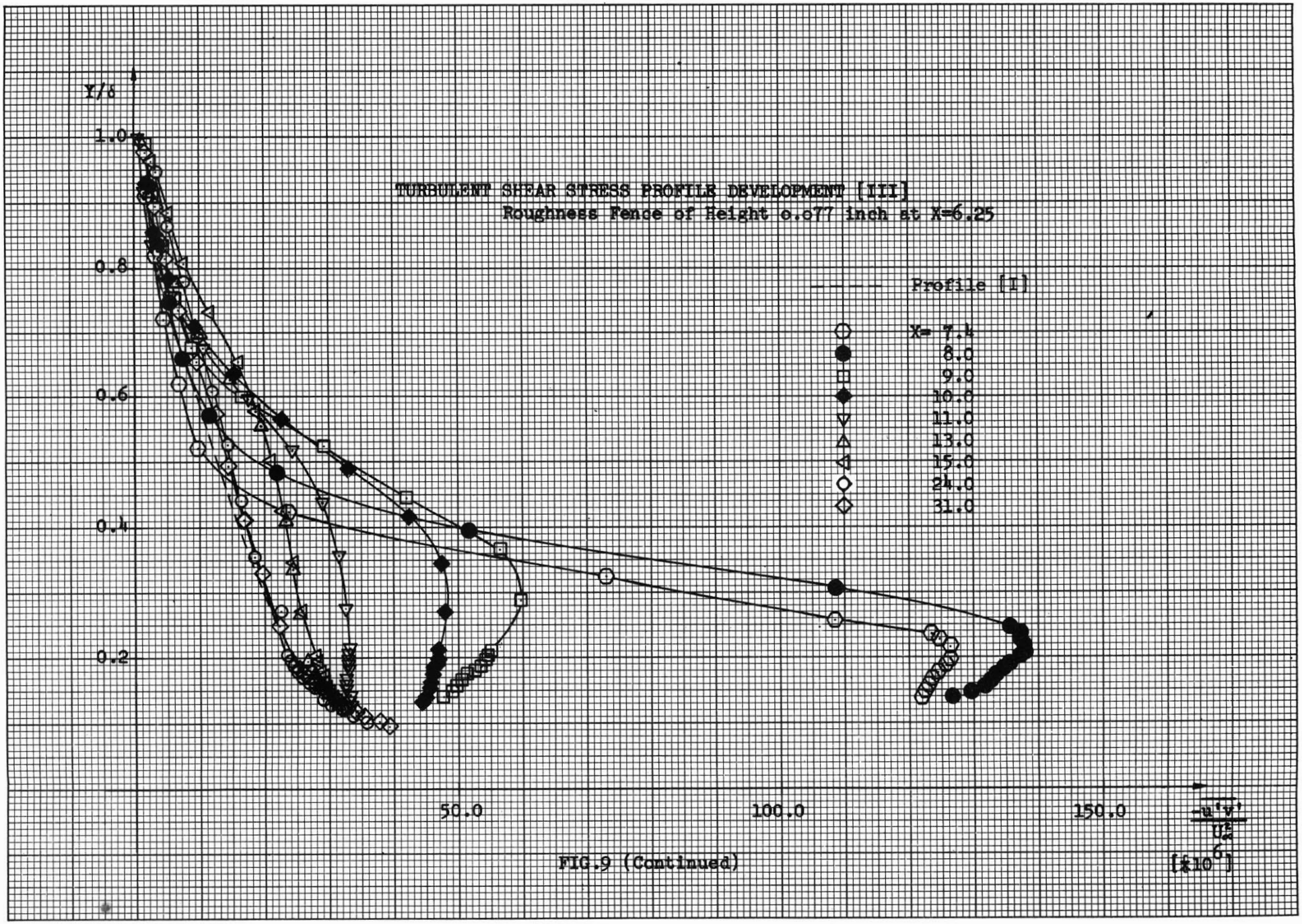

FIG.9 (Continued)

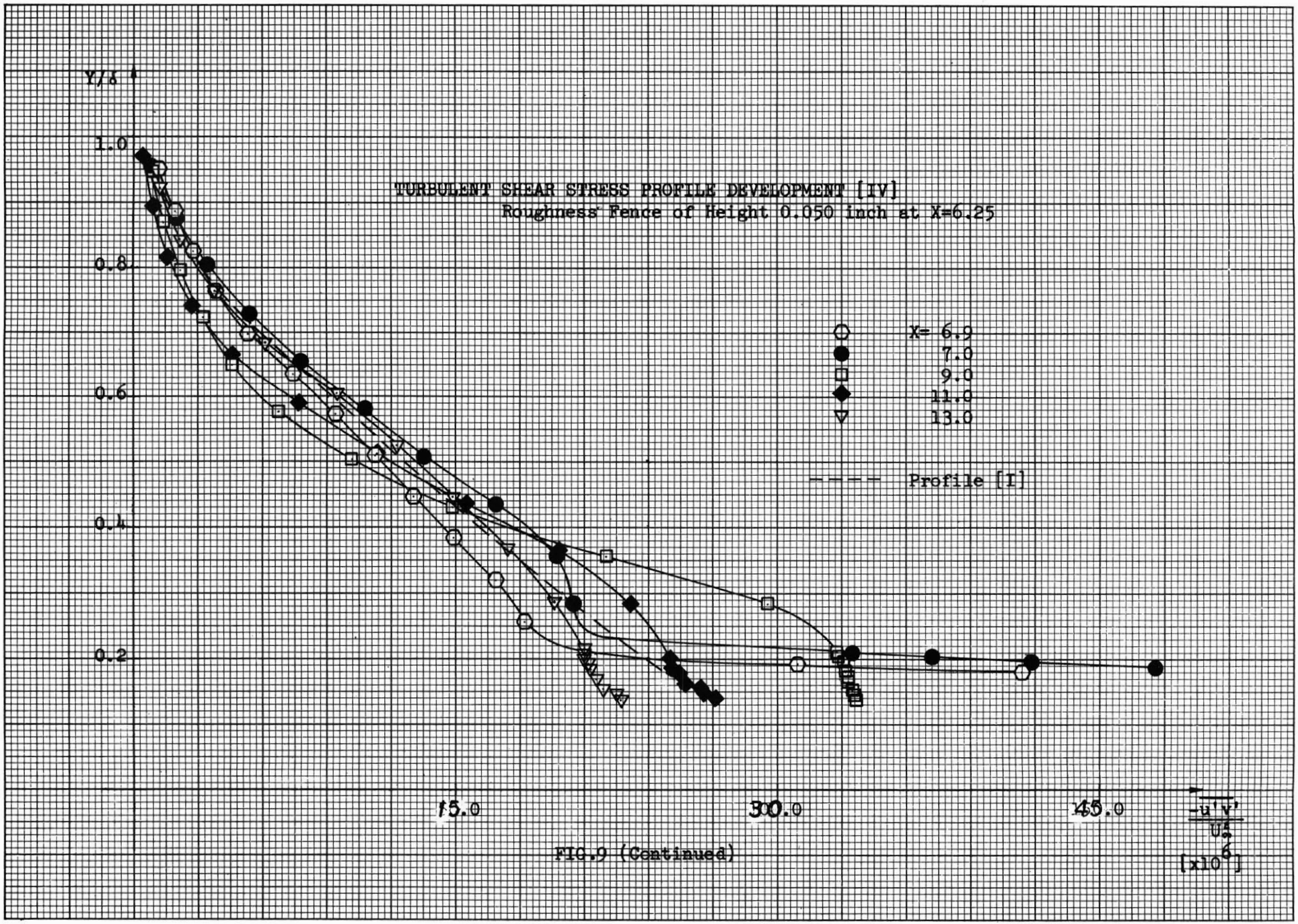

FIG.9 (Continued)

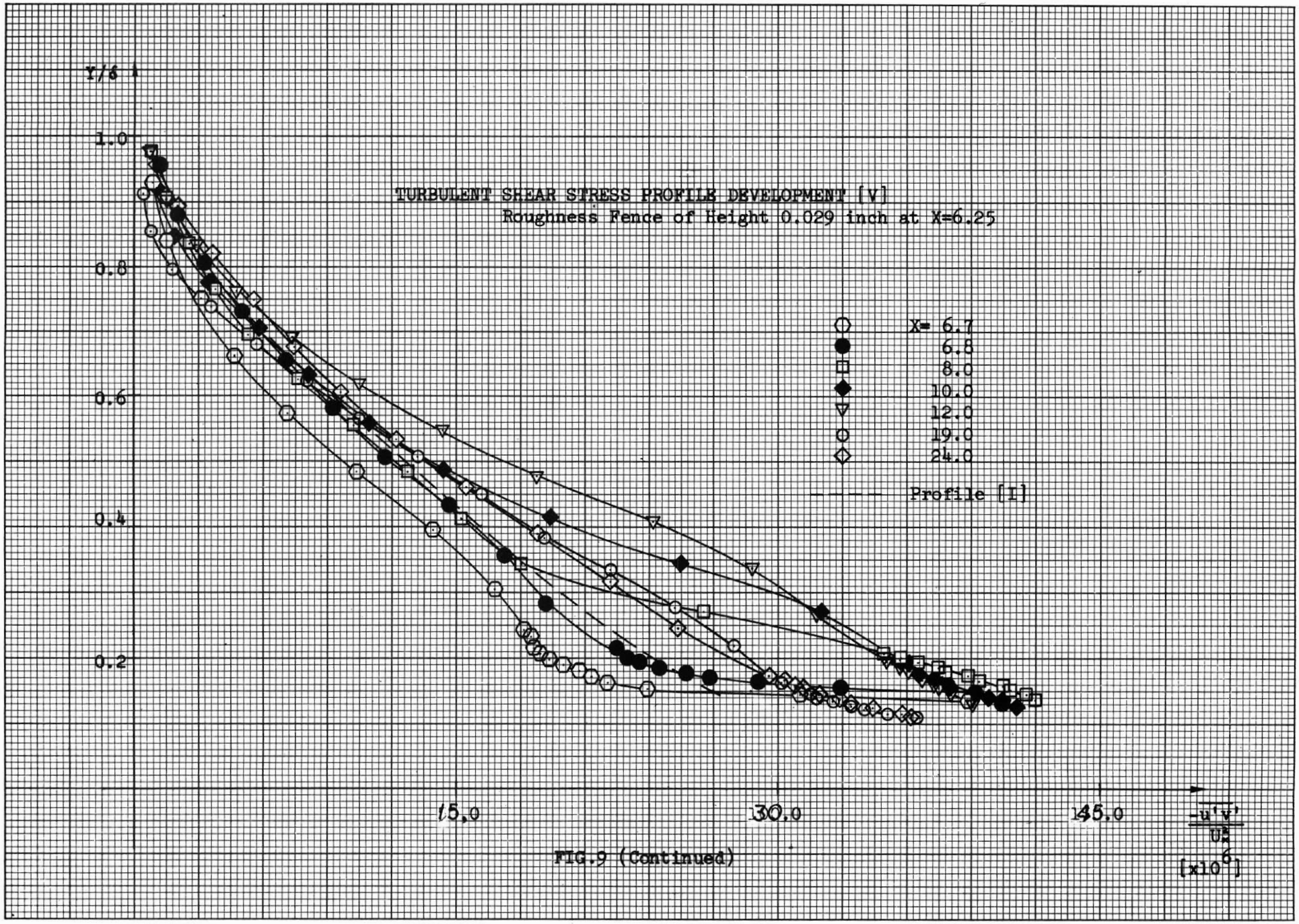

FIG.9 (Continued)

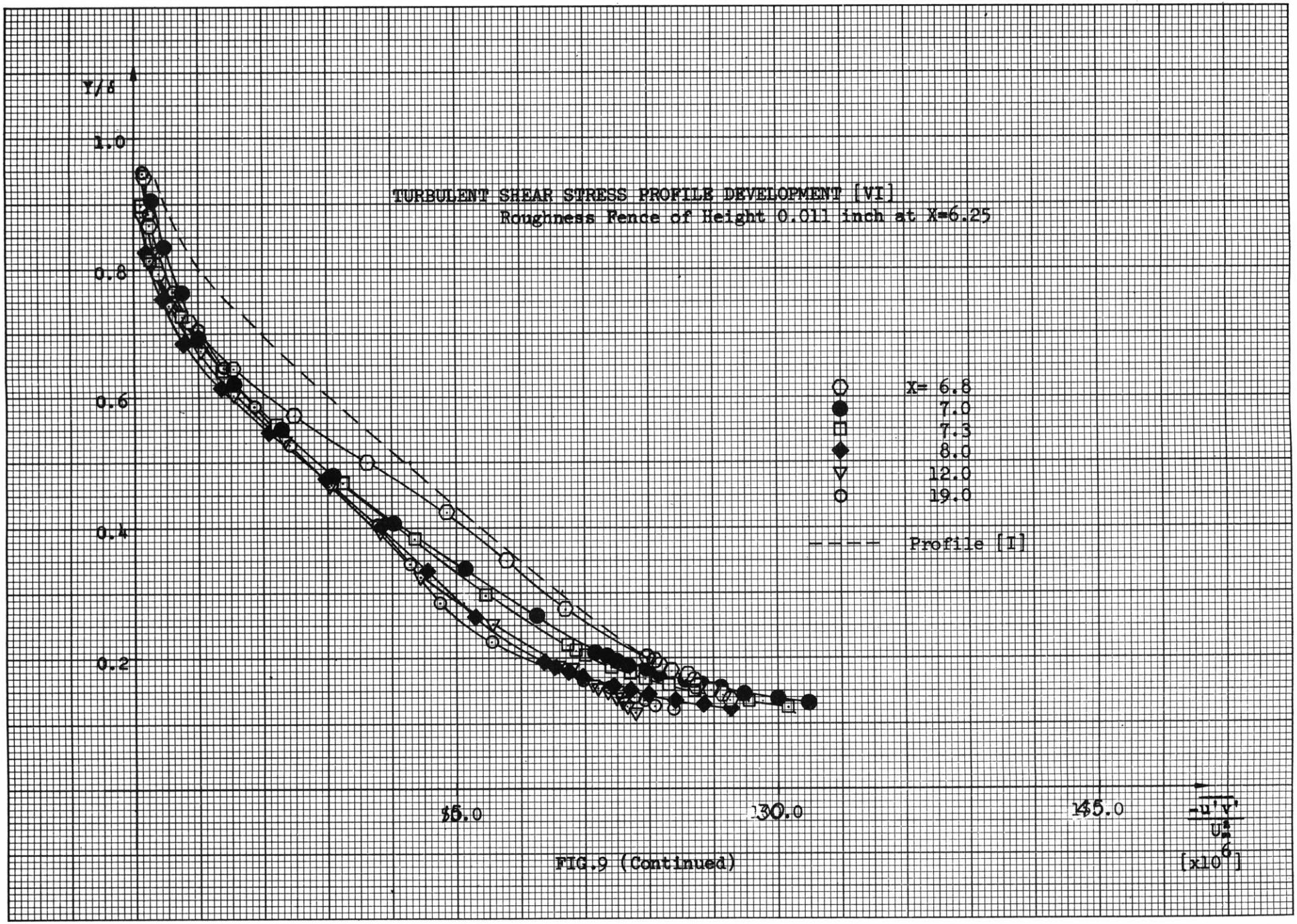

FIG.9 (Continued)

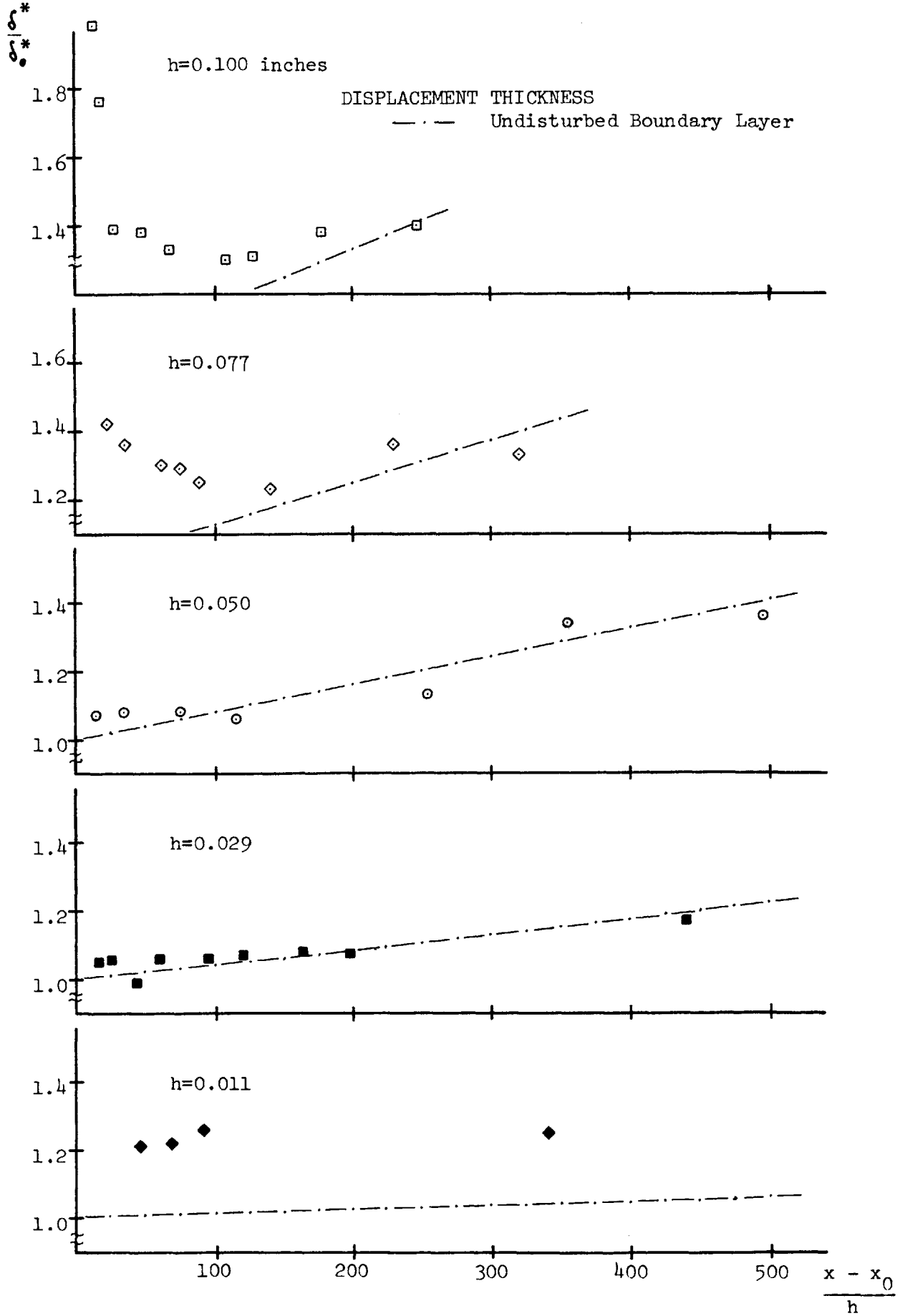
δ*/δ*₀
h=0.100 inches
DISPLACEMENT THICKNESS
Undisturbed Boundary Layer
1.8
1.6
1.4
h=0.077
1.6
1.4
1.2
h=0.050
1.4
1.2
1.0
h=0.029
1.4
1.2
1.0
h=0.011
1.4
1.2
1.0
100
200
300
400
500
x - x0
h

FIG.10

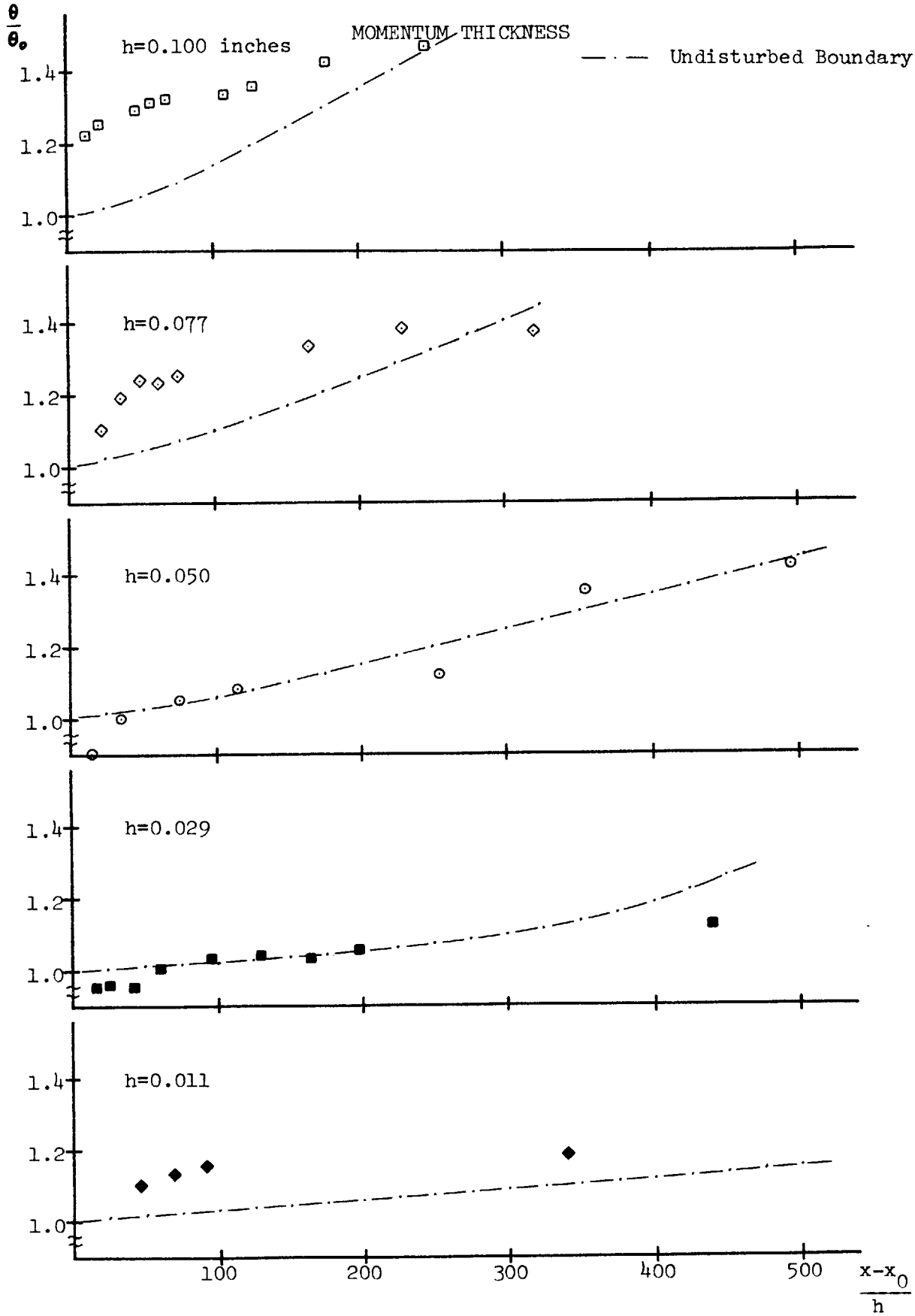
θ/θ₀
MOMENTUM THICKNESS
h=0.100 inches
Undisturbed Boundary Layer
h=0.077
h=0.050
h=0.029
h=0.011
1.0
1.2
1.4
100
200
300
400
500
x-x₀/h

FIG.11

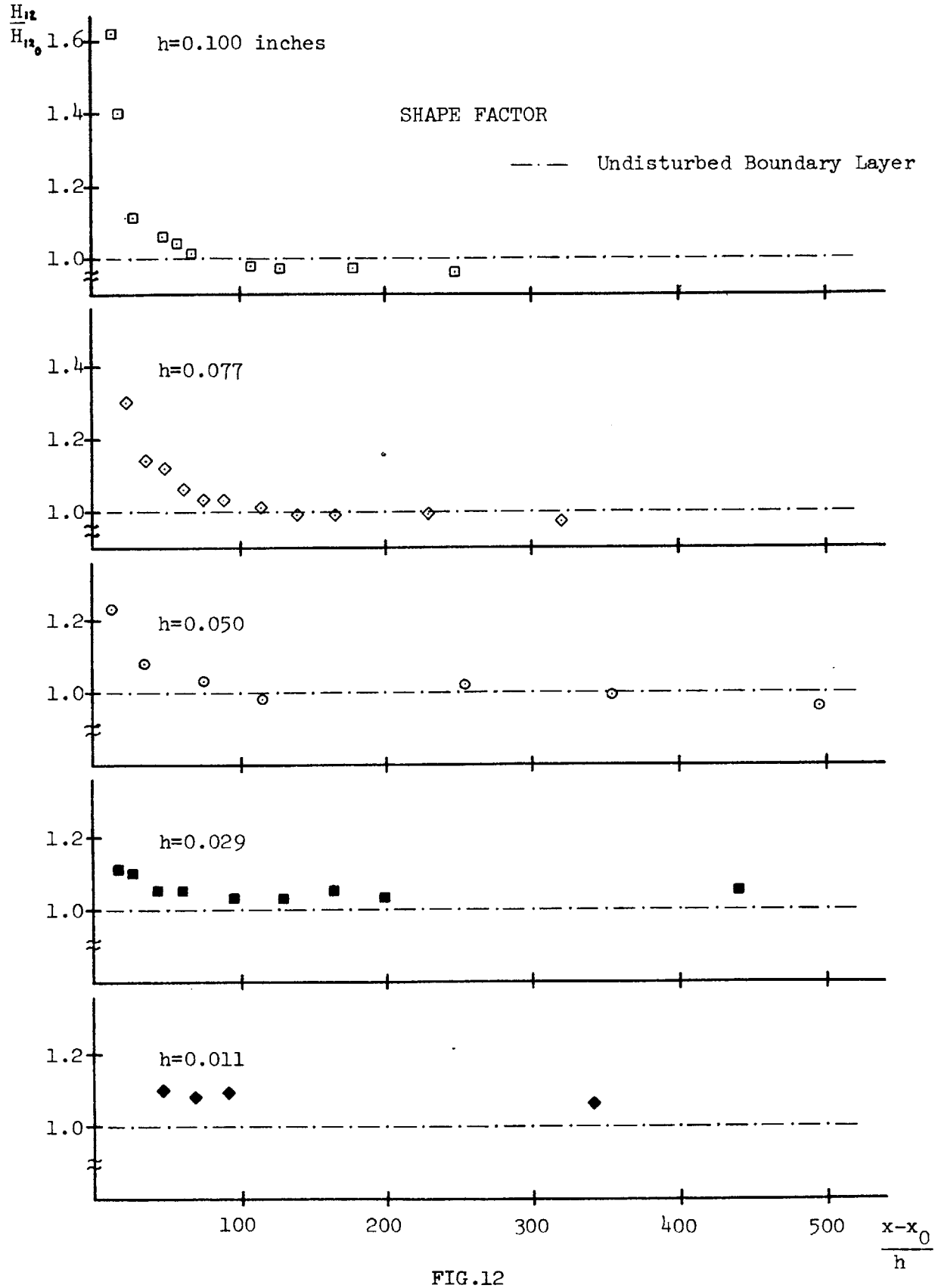
$\frac{H_{12}}{H_{12_0}}$
h=0.100 inches
SHAPE FACTOR
Undisturbed Boundary Layer
h=0.077
h=0.050
h=0.029
h=0.011
1.6
1.4
1.2
1.0
100
200
300
400
500
$\frac{x-x_0}{h}$

FIG.12

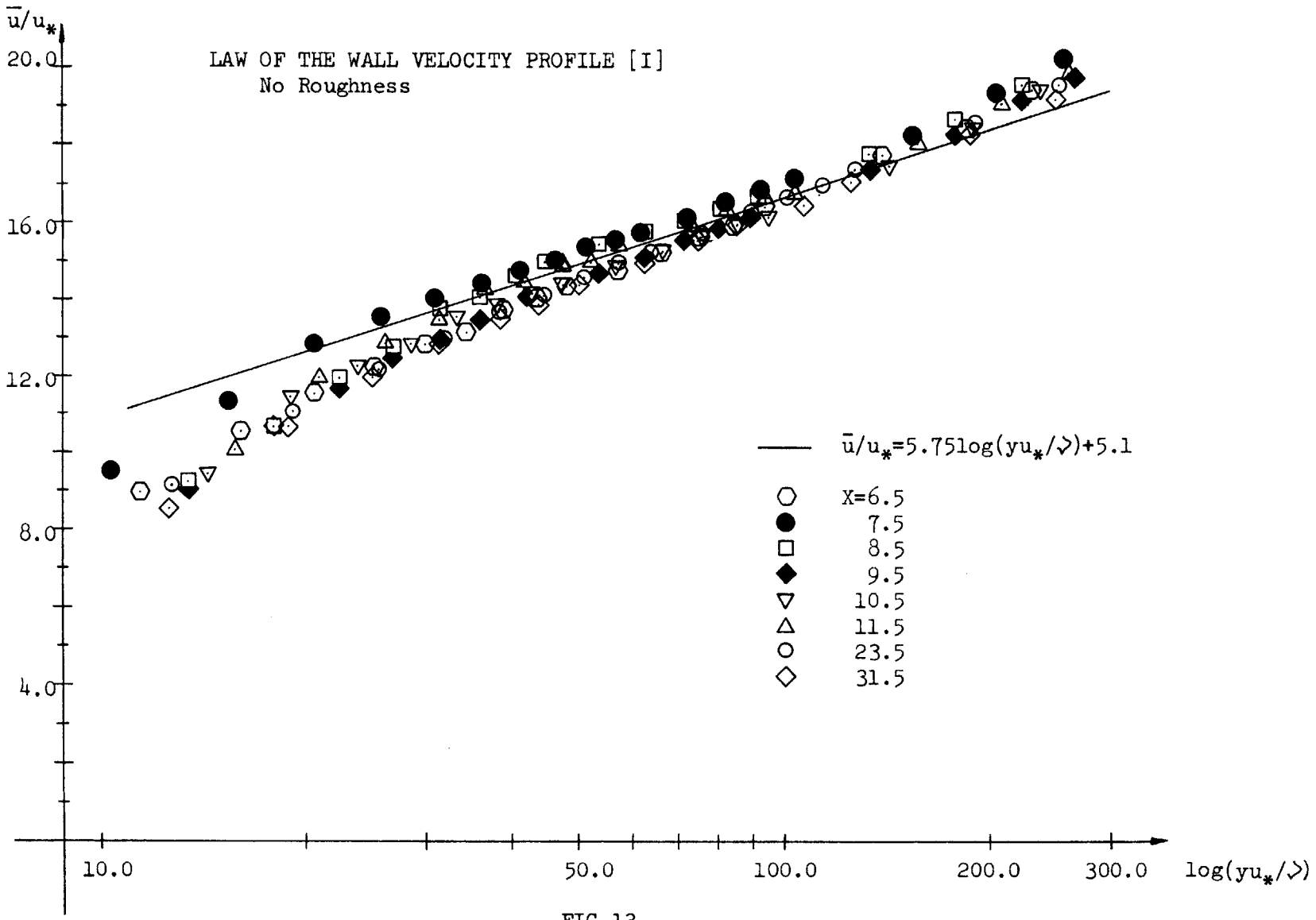
$\bar{u}/u_*$
LAW OF THE WALL VELOCITY PROFILE [I]
No Roughness
20.0
16.0
12.0
8.0
4.0
10.0
50.0
100.0
200.0
300.0
$\log(yu_*/\nu)$
$\bar{u}/u_*=5.75\log(yu_*/\nu)+5.1$
X=6.5
7.5
8.5
9.5
10.5
11.5
23.5
31.5

FIG.13

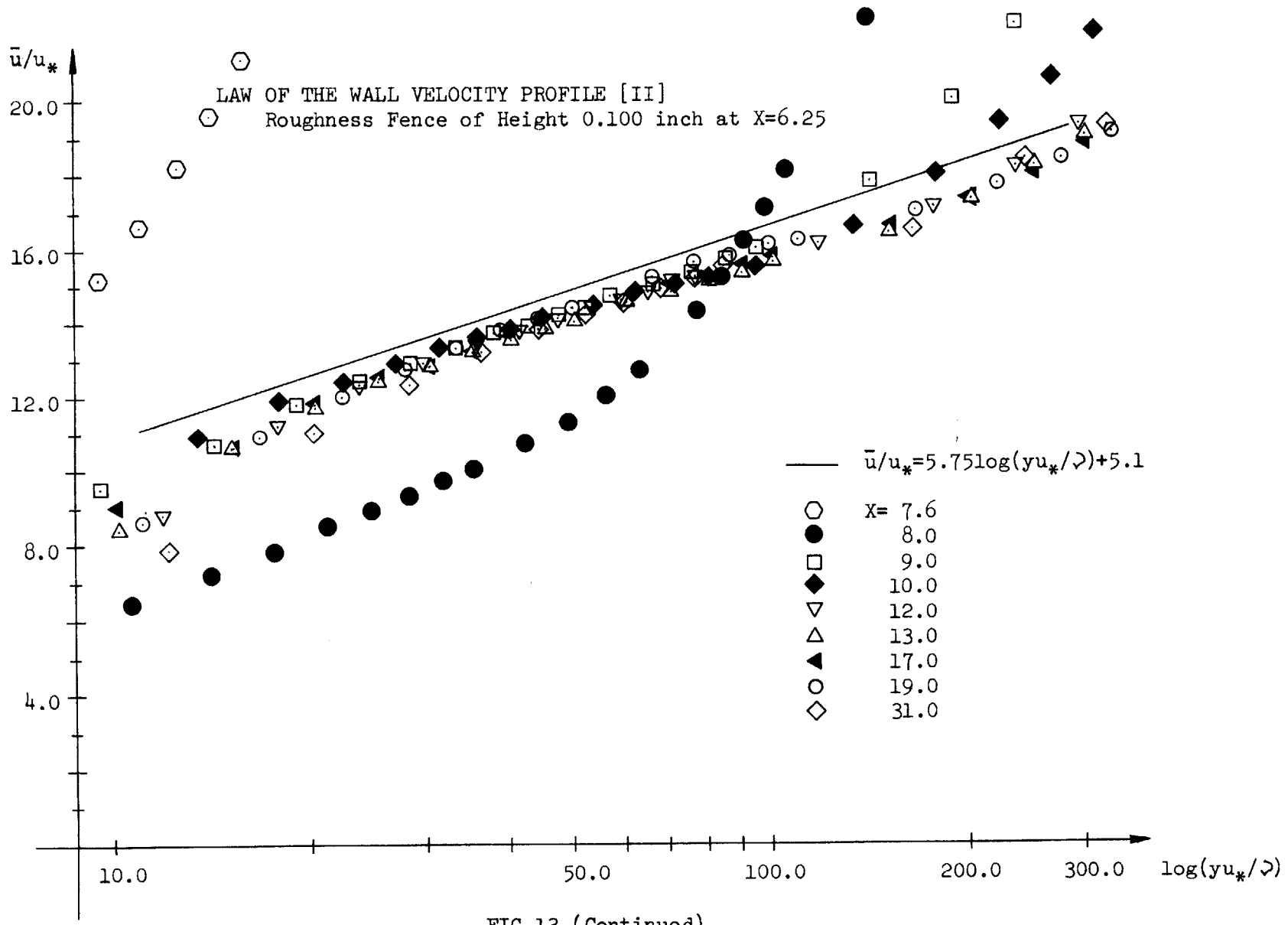

FIG.13 (Continued)

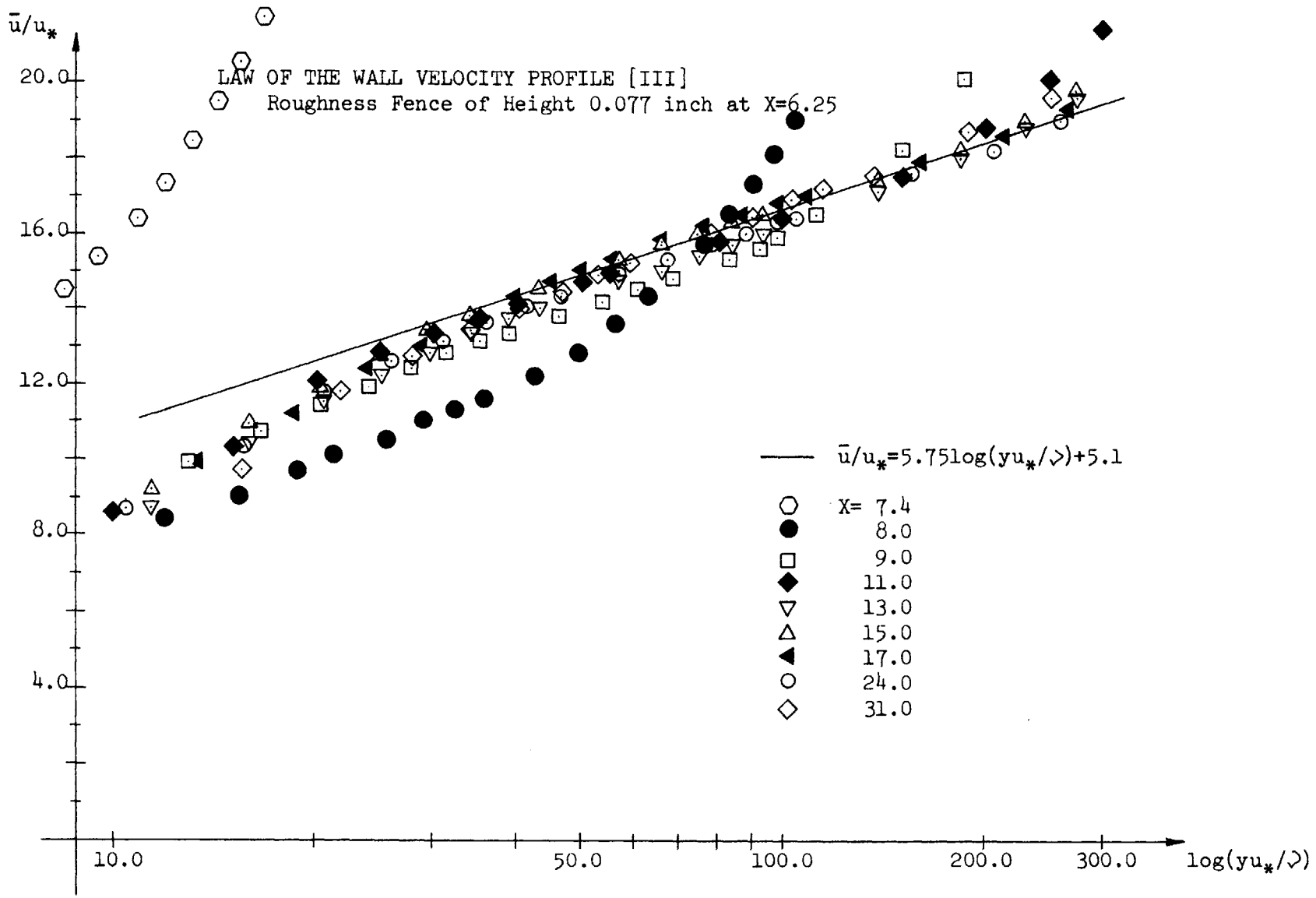

FIG.13 (Continued)

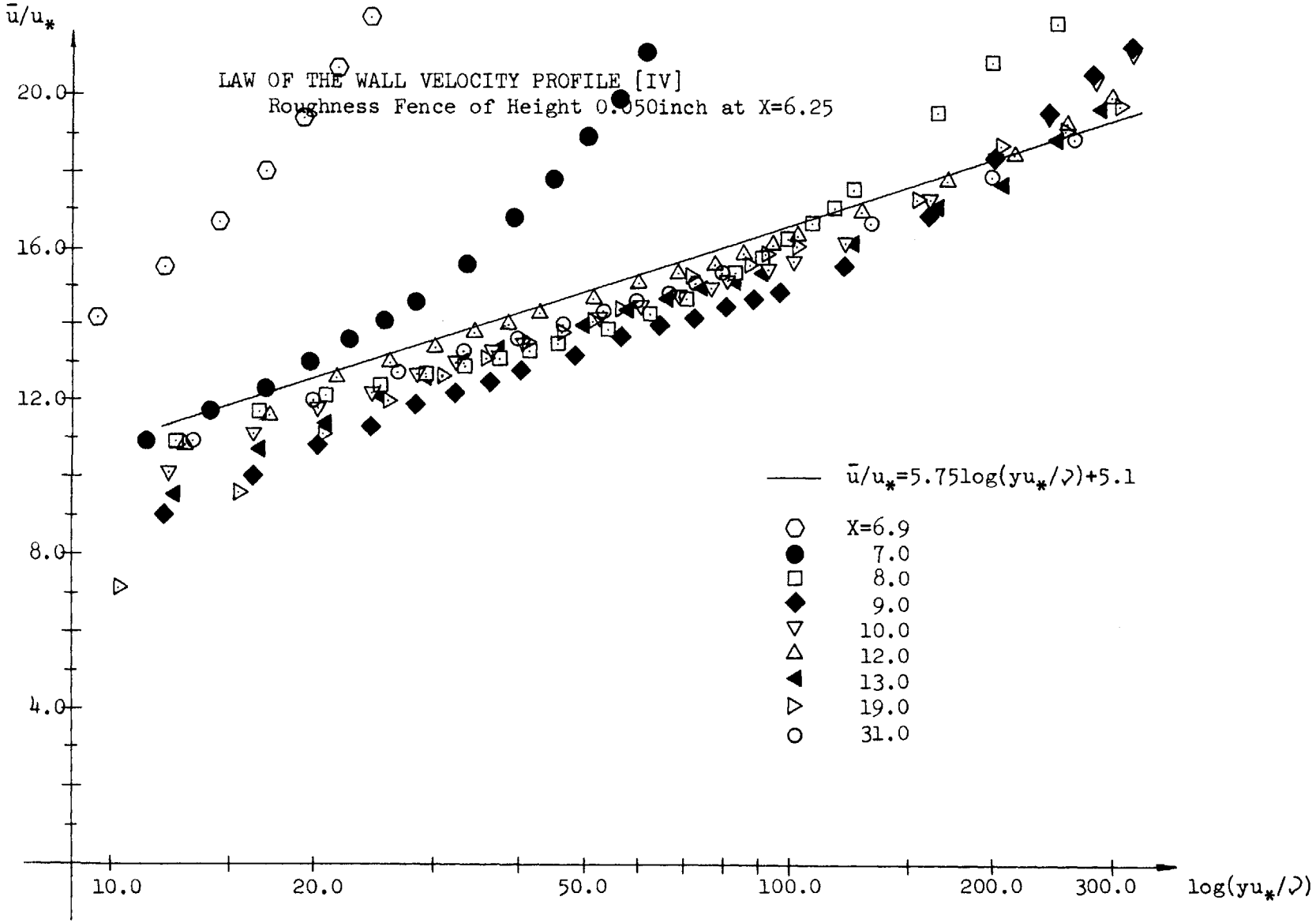

FIG.13 (Continued)

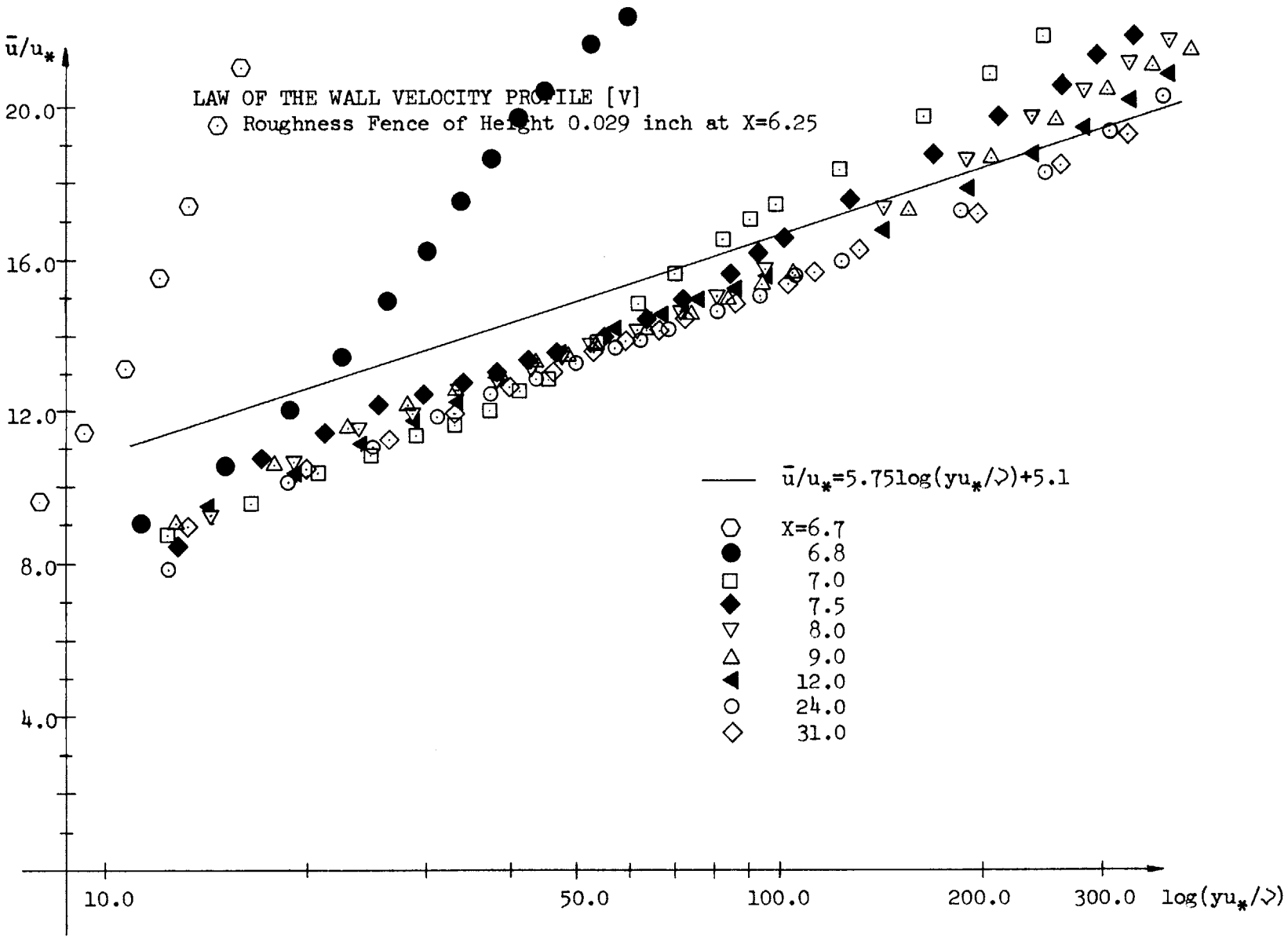

FIG.13 (Continued)

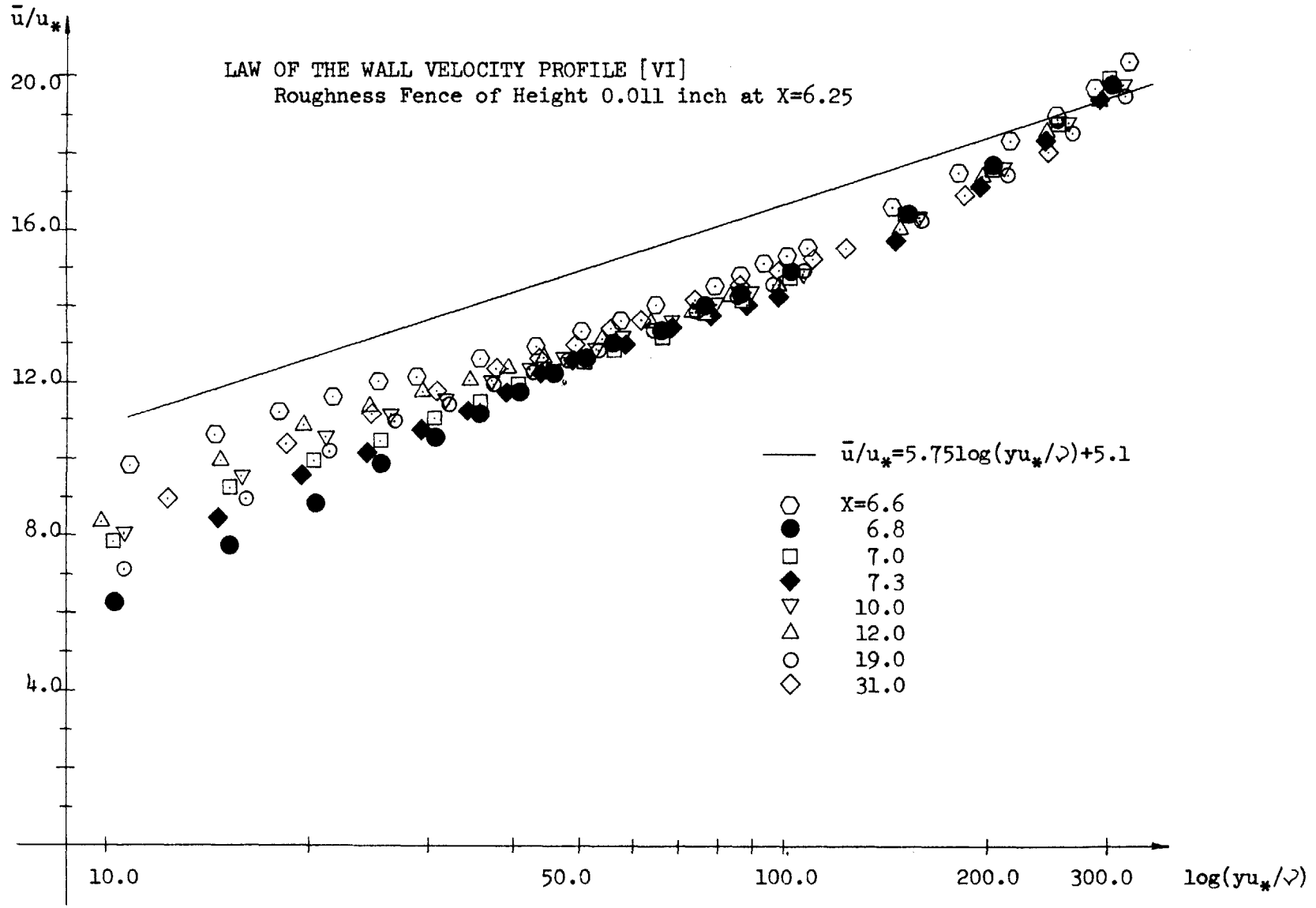

FIG.13 (Continued)

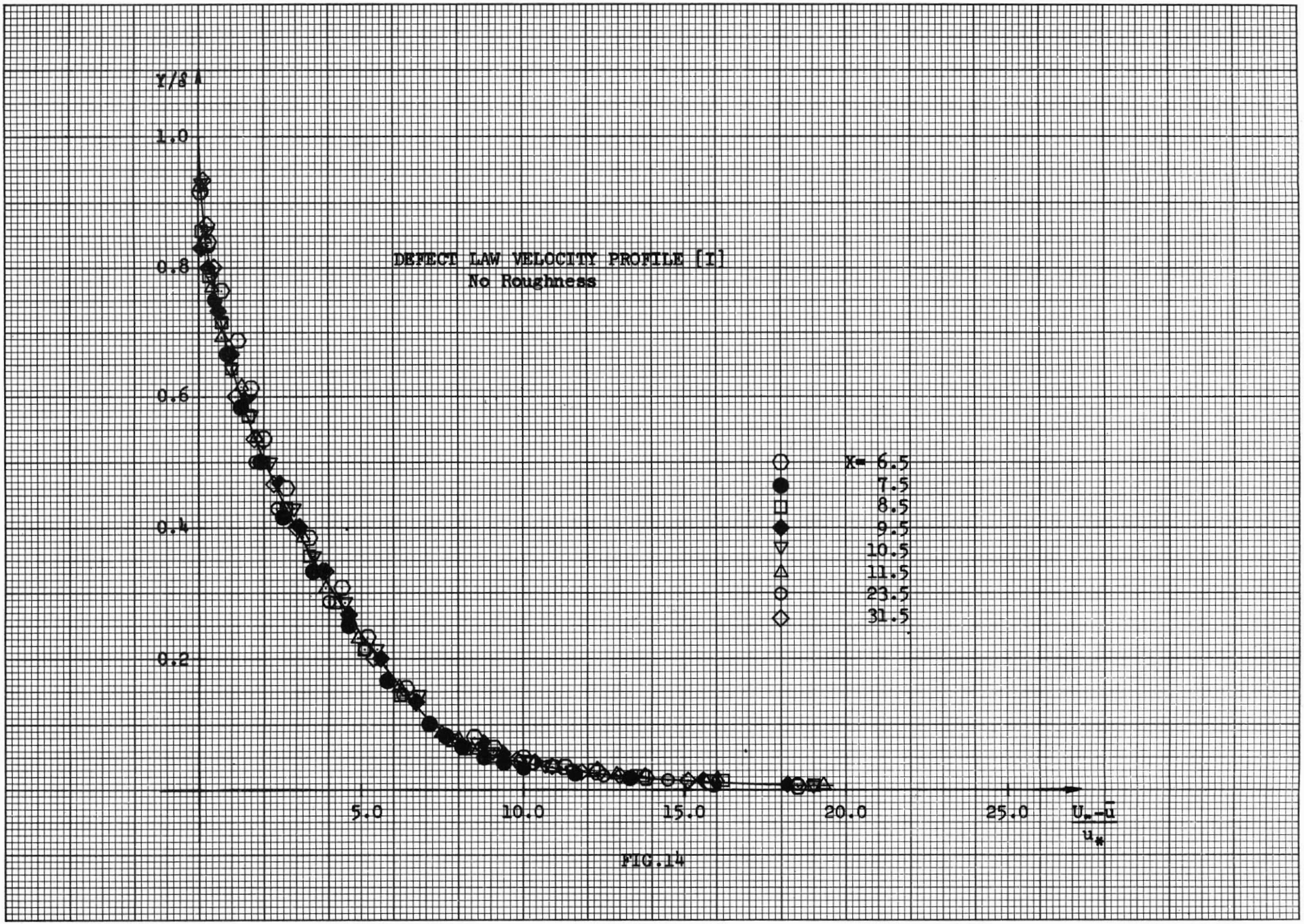
Y/δ
1.0
0.8
0.6
0.4
0.2
DEFECT LAW VELOCITY PROFILE [I]
No Roughness
X= 6.5
7.5
8.5
9.5
10.5
11.5
23.5
31.5
5.0
10.0
15.0
20.0
25.0
U∞-ū / u*

FIG.14

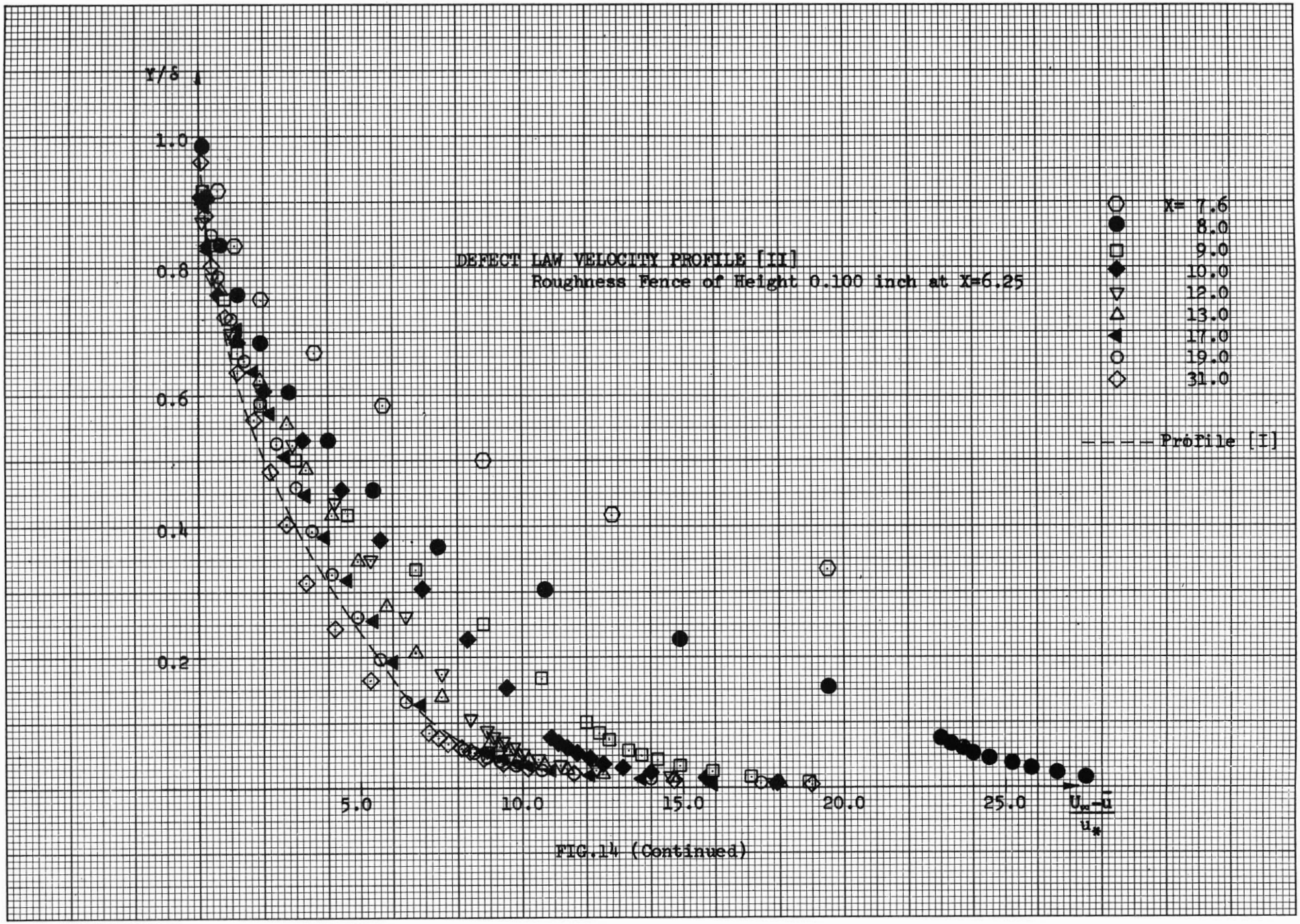

FIG.14 (Continued)

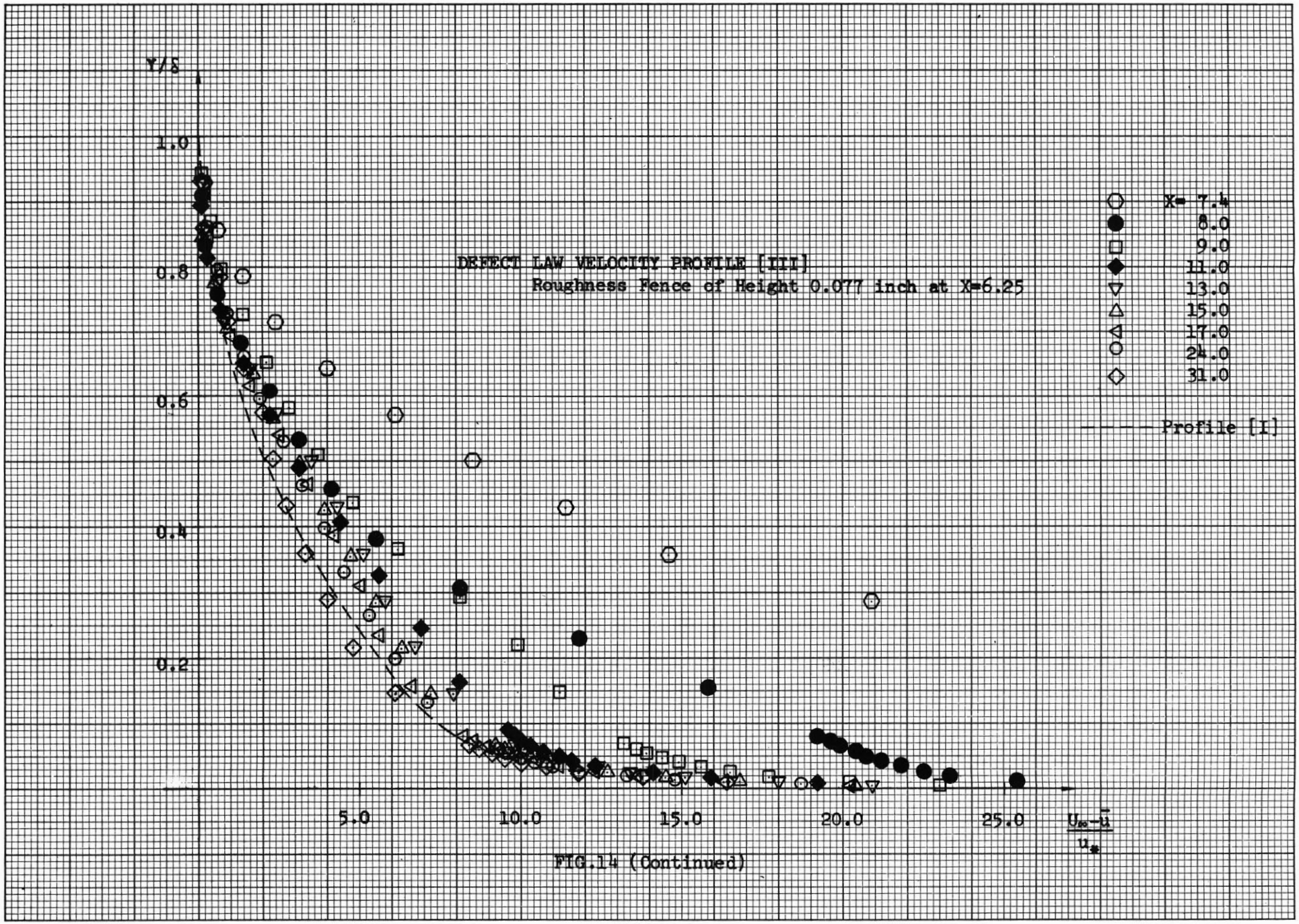

FIG.14 (Continued)

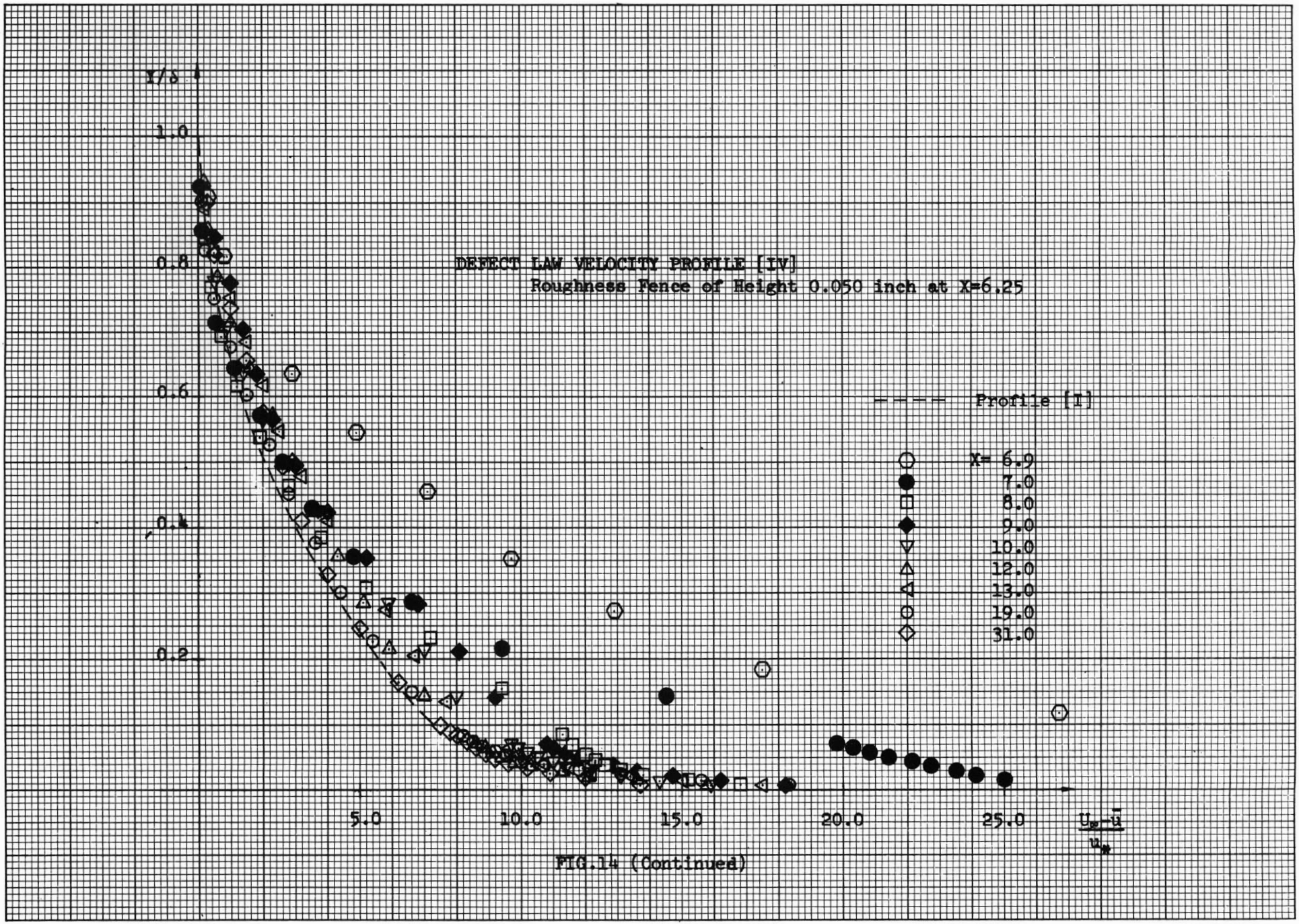

FIG.14 (Continued)

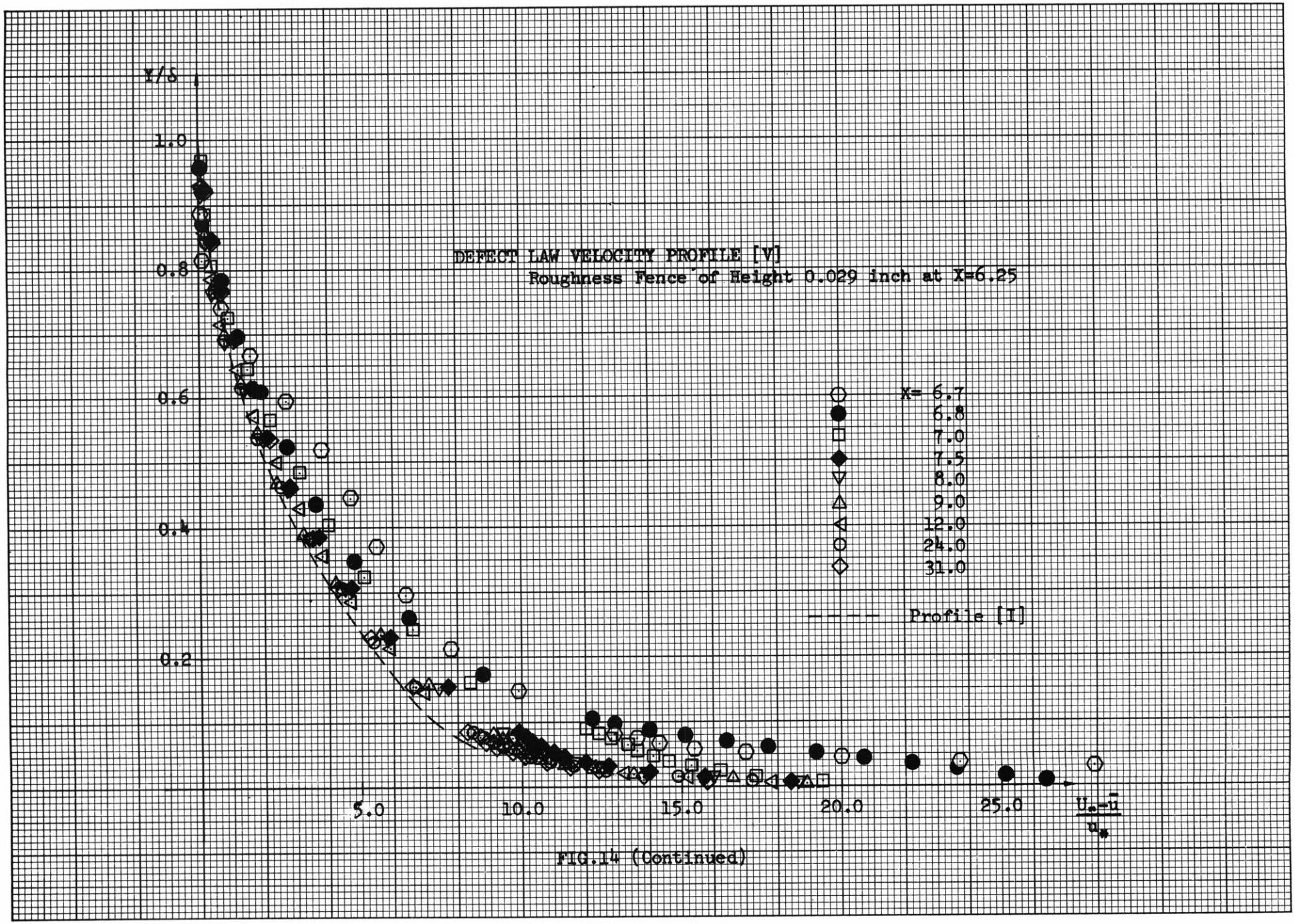

FIG.14 (Continued)

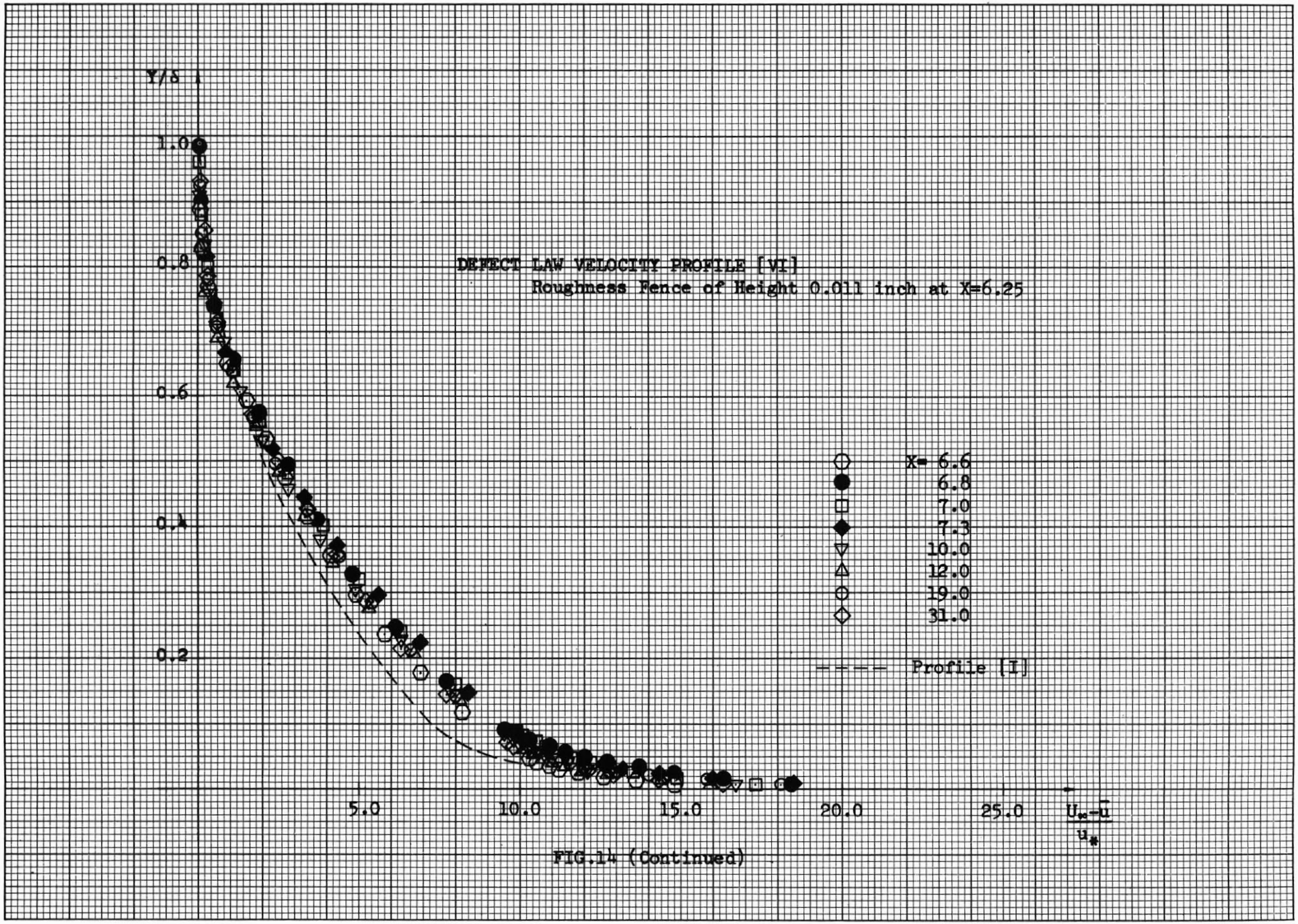

FIG.14 (Continued)

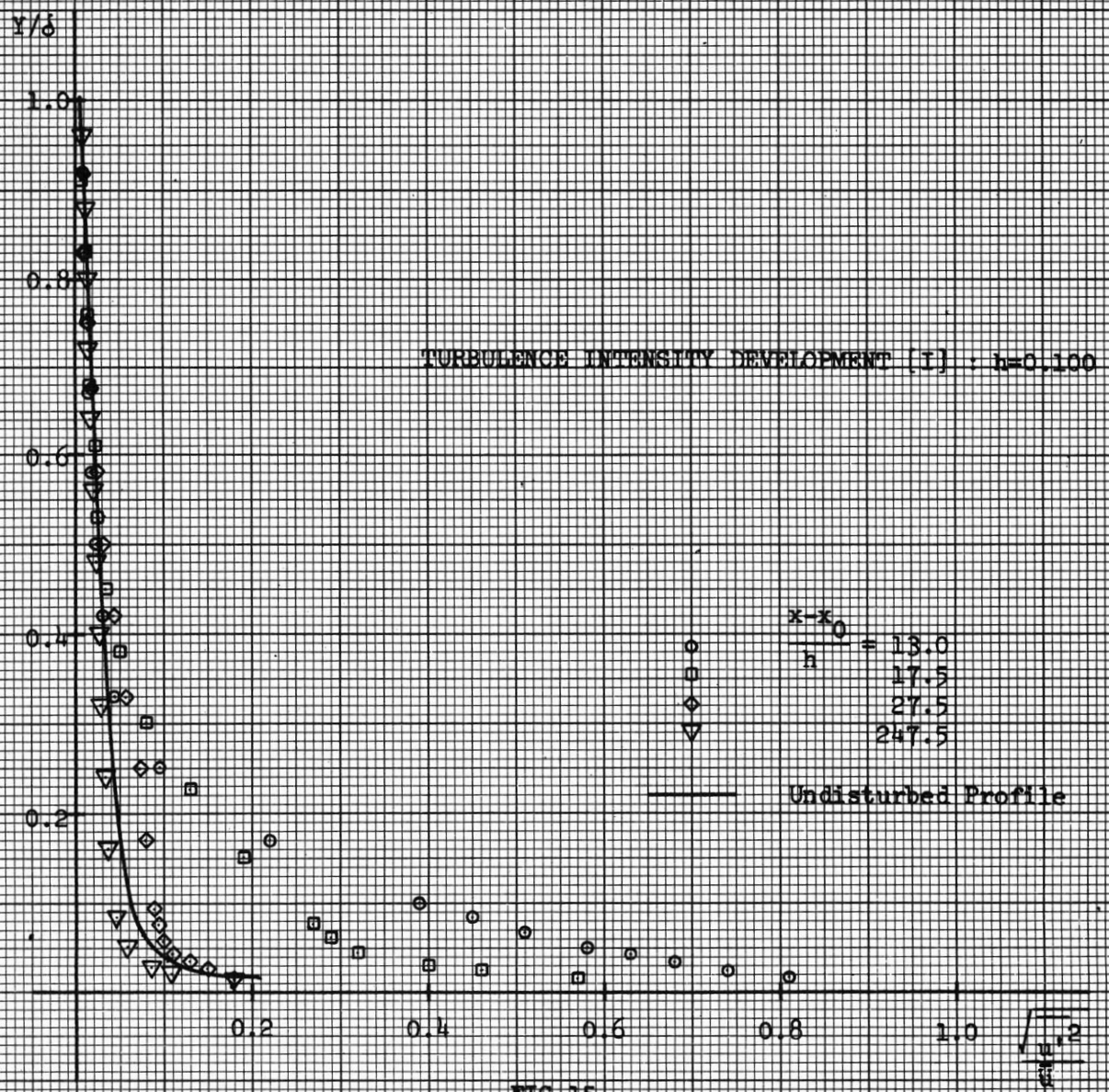
Y/δ
1.0
0.8
0.6
0.4
0.2
0.2
0.4
0.6
0.8
1.0
TURBULENCE INTENSITY DEVELOPMENT [I] : h=0.100 inches
(x-x0)/h = 13.0
17.5
27.5
247.5
Undisturbed Profile

FIG.15

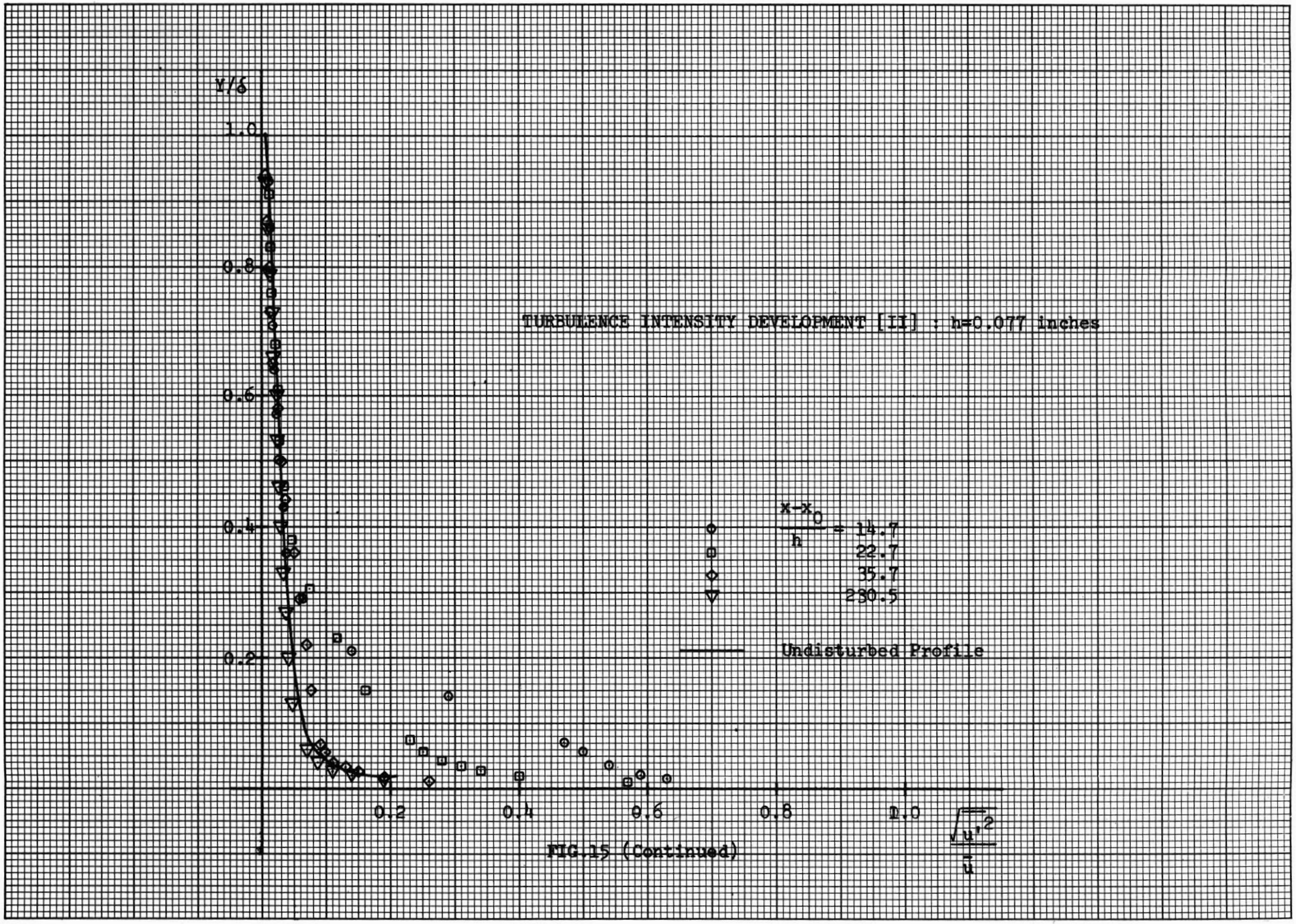

FIG.15 (Continued)

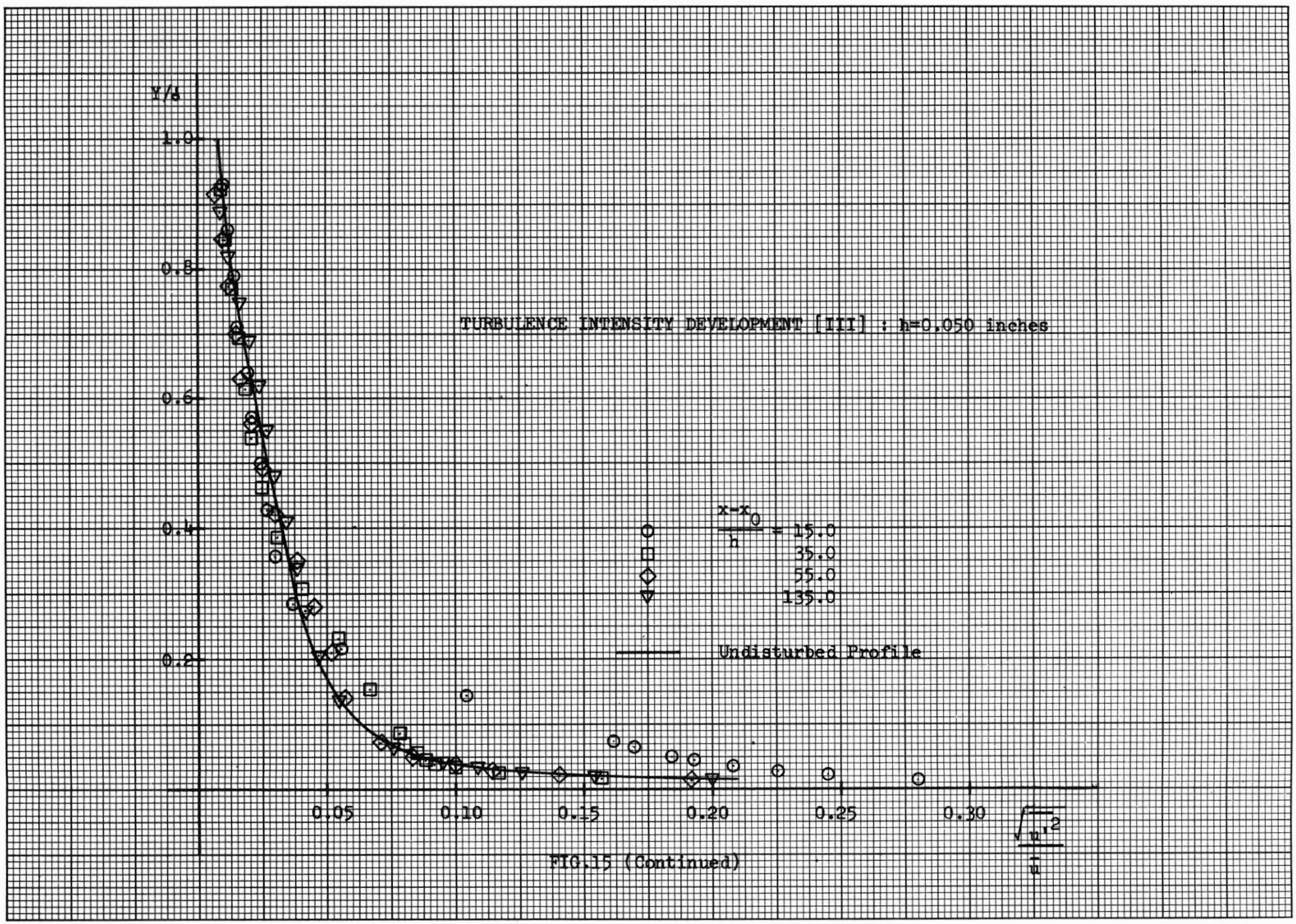

FIG.15 (Continued)

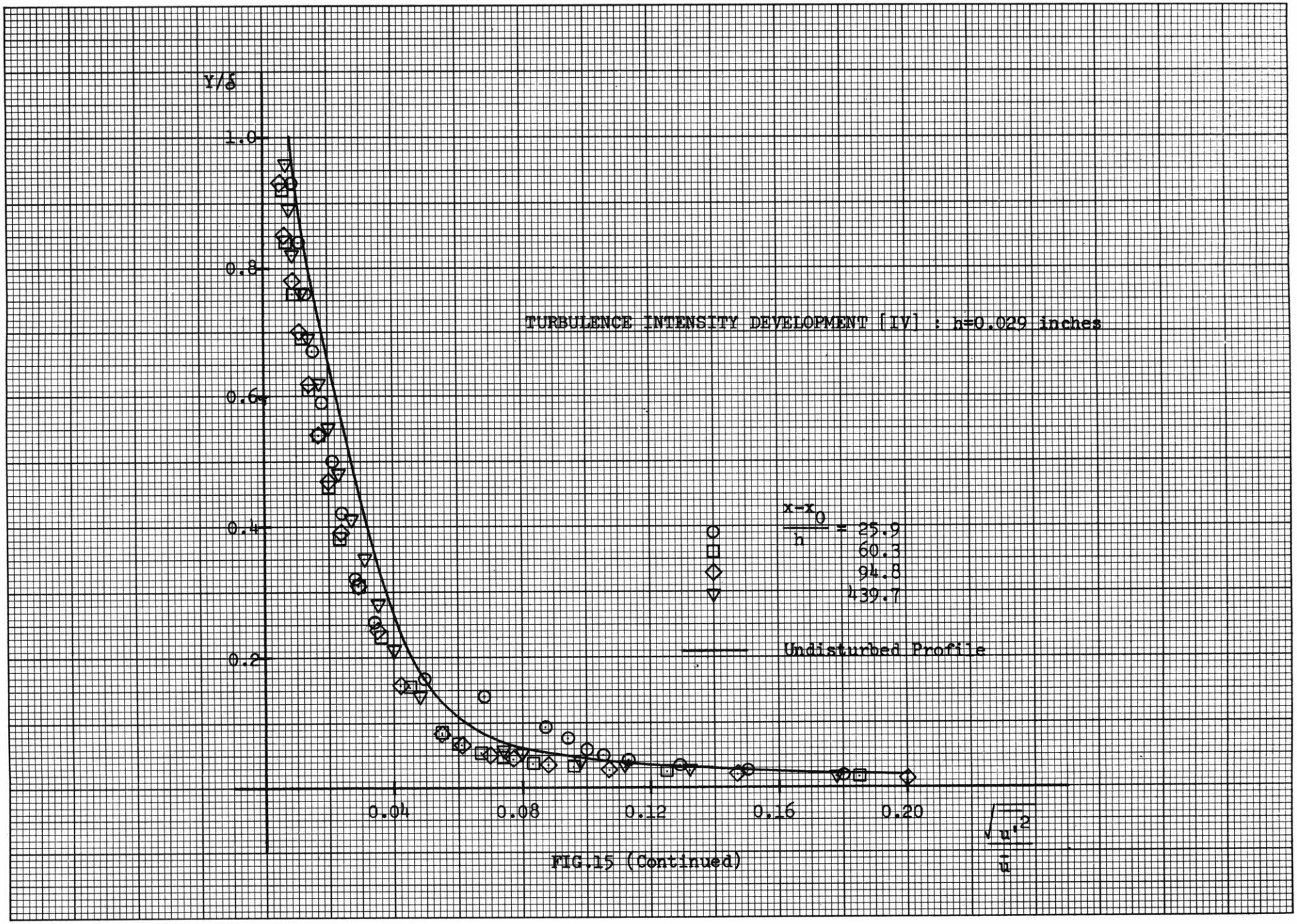

FIG.15 (Continued)

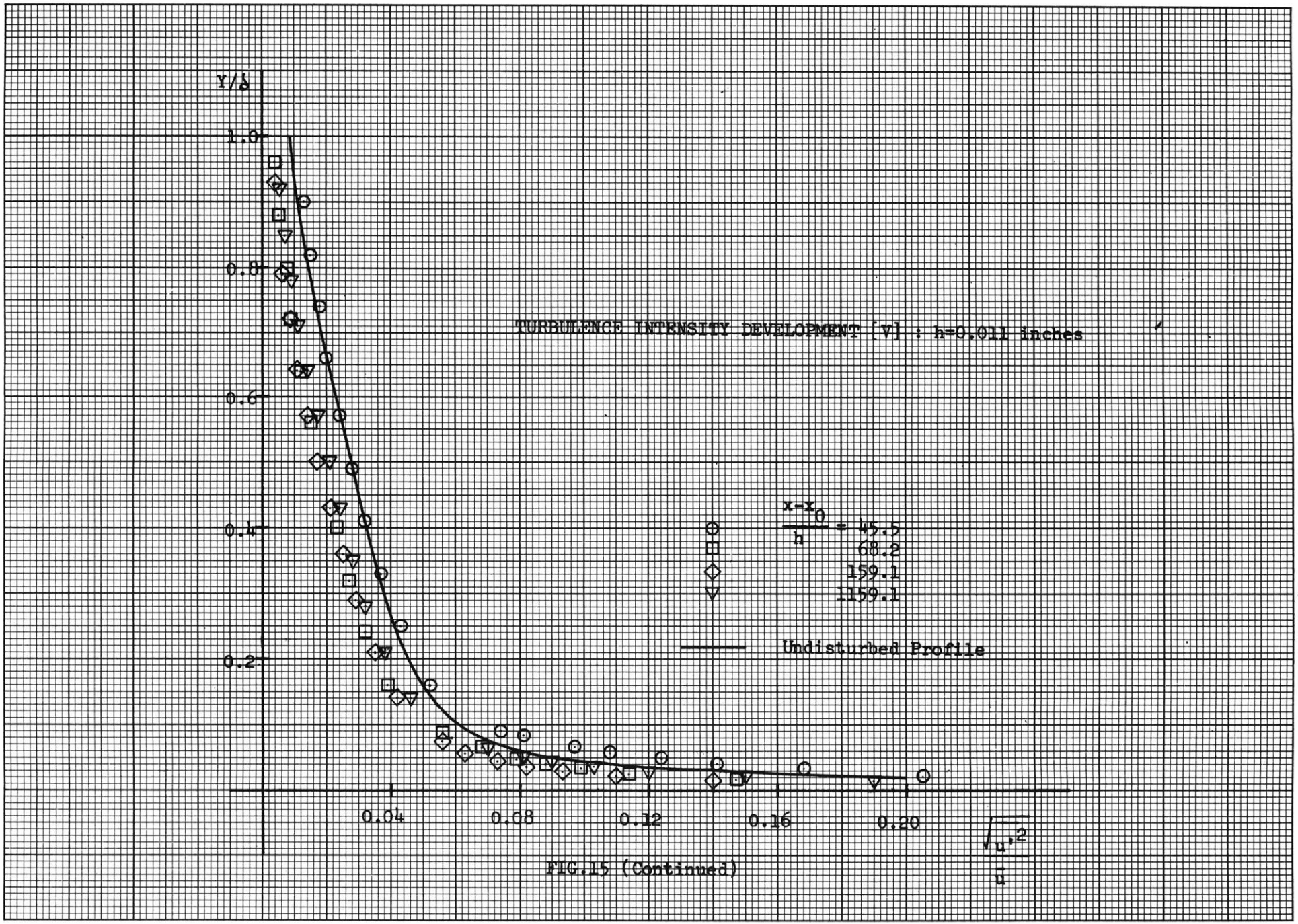

FIG. 15 (Continued)